Filipe Tadeu Alves Tiago

Degree in Biology

Using CRISPR-Cas9 technology to create *Danio rerio dnah7* mutants

A thesis submitted in fulfillment of the requirements for the degree of the Masters in Molecular Genetics and Biomedicine

Supervisor: Susana Santos Lopes, PhD, CEDOC-FCM

FACULDADE DE CIÊNCIAS E TECNOLOGIA
UNIVERSIDADE NOVA DE LISBOA

September, 2017

Filipe Tadeu Alves Tiago

Degree in Biology

Using CRISPR-Cas9 technology to create *Danio rerio dnah7* mutants

A thesis submitted in fulfillment of the requirements for the degree of the Masters in

Molecular Genetics and Biomedicine

September, 2017

Using CRISPR-Cas9 technology to create *Danio rerio dnah7* mutants

Acknowledgments

First of all, I would like to thank my supervisor, Susana Lopes, for giving this amazing opportunity to learn and to do my Master thesis in her Cilia Regulation and Disease Laboratory. She was supportive and a great teacher all throughout my stay in CEDOC. It was a great honor to have worked under her leadership.

I also want to thank to all my colleges in the Lab. I'm very grateful to Monica, Pedro, Sara and Raquel for all the support given in the high and lows of my thesis and for the constructive criticism. I can surely say that Raquel was the best mentor that a Master student can ask for, her patience, support and ability to lead were truly amazing and for that I'm forever thankful. Likewise, I cannot forget Catarina, Inês and Margarida for all the wonderful moments passed together during our thesis dissertation.

A special mention to Domino´s pizza Areeiro for teaching me the value of working hard and that perseverance is always rewarded in a way on the other.

I also would like to thank Filipa for the support and inspiration to keep going.

Finally, a more than special thank you to my mother and father that allowed me to have this opportunity in the first place. Their efforts to make sure that I have a good education will be forever valued. Furthermore, their relentless support throughout my life and this year was what got me through having a job and a thesis dissertation. Thank you for all of that.

Abstract

CRISPR-Cas9 is a recent discovered genetic editing mechanism, that shows a lot of versatility. This allows scientists to do genetic manipulation with relative ease when compared with others current genetic tools available. One possible application of the CRISPR-Cas9 system is to mimic human disease mutations by targeting orthologous genes in animal models, which allows a better characterization of the mechanisms behind a particular disease.

Cilia are hair-like structures that protrude from the cell surface in organisms and can be classified as motile or non-motile. They are responsible for several important functions throughout the human body. Such functions include, generating fluid flow and sensing mechanical or chemical cues from the surrounding environment. If these are compromised it can lead to ciliopathies. Ciliopathies are a group of diseases and syndromic diseases characterized by malfunctioning of cilia. Motile cilia can lead to a disease known as primary ciliary dyskinesia (PCD). More than 35 genes have been linked with cilia motility in PCD patients. Some of these genes are associated with the inner dynein arms present in the axoneme. A better understanding of mutations in these genes would help the characterization of PCD.

Using CRISPR-Cas9 we tried to cause a mutation in *dnah7*, a gene that encodes a protein present in inner dynein arms. Two SgRNAs were selected to disrupt *dnah7* and injected into zebrafish embryos. These F0 embryos were screened for mutations outcrossed and left to sexually mature. When matured, the progeny was screened again to find any heritable mutations. Meanwhile, analyses of cilia beat frequency and pattern, the readouts of cilia function, were made in a set of wild type and *ccdc40* MO injected zebrafish. Additionally, two SgRNAs were designed for targeting another PCD commonly mutated gene named *rsph4a*, a gene coding for a protein present in the radial spokes of the axonemes.

Key words: CRISPR-Cas9, Cilia, SgRNAs, *Danio rerio* (Zebrafish), Primary Ciliary Dyskinesia (PCD), Cilia Beat Frequency (CBF)

Resumo

CRISPR-Cas9 foi recentemente descoberto como um mecanismo de edição genética que mostra bastante versatilidade. Isto permite aos cientistas fazerem manipulações genéticas com extrema facilidade quando comparado com outras ferramentas genéticas atualmente disponíveis. Uma aplicação possível com o sistema CRISPR-Cas9 é a criação de mutações que mimetizem doenças humanas em animais modelo o que permite uma melhor caracterização dos mecanismos subjacentes de uma determinada doença.

Cílios são estruturas parecidas com pestanas, que saem da superfície da célula e que são classificados como móveis ou imóveis. Os cílios são responsáveis por realizar inúmeras funções no corpo, como a geração de fluidos e detecção de sinais mecânicos ou químicos no ambiente circundante. Se estas funções forem comprometidas podem originar ciliopatias. As ciliopatias são um grupo de doenças caracterizadas por defeitos ciliares. Os cílios moveis podem originar uma doença conhecida como discinesia ciliar primária (DCP). Mais de 35 genes foram relacionados a defeitos de mobilidade dos cílios de pacientes de DCP. Alguns destes genes estão associados aos braços de dineína internos do axonema. Uma melhor compreensão das mutações nesses genes ajudaria na caracterização da doença.

Através do uso de CRISPR-Cas9 tentei criar uma mutação no gene *dnah7*, este gene codifica para uma proteína presente nos braços de dineína internos. Dois RNAs guias foram selecionados para danificar *dnah7* e foram injetados em embriões de peixe-zebra. Uma triagem em embriões F0 foi feita para a detecção de mutações nos peixes que posteriormente foram deixados para maturarem sexualmente. Após esse período, foram feitas triagens para detetar mutações hereditárias. Entretanto foi conduzida uma análise ao batimento ciliar entre peixes selvagens e peixes injetados com *ccdc40*. Para além disso, dois novos RNAs guias foram selecionados para *rsph4a*. Este gene codifica para uma proteína presente no axonema e mutações neste gene já foram identificadas em vários doentes de DCP.

Palavras-chave: CRISPR-Cas9, Cílios, SgRNAs, *Danio rerio* (Peixe zebra), Discinesia ciliar primária (DCP), Batimento ciliar

General Index

List of Figures

List of tables

List of abbreviations and acronyms

ALMS - Alström Syndrome

BBS - Bardet−Biedl Syndrome

CBF - Cilia beat frequency

Ccdc39 - Coiled-coil domain containing 39

Ccdc40 - Coiled-coil domain containing 40

CP - Central pair

CRISPR - Clustered regularly interspaced short palindromic repeats

CrRNA - CRISPR DNA

D-loop - Displacement-loop

DNA - Deoxyribonucleic acid

Dnah5 - Dynein axonemal heavy chain 5

Dnah7 - Dynein axonemal heavy chain 7

Dnah11 - Dynein axonemal heavy chain 11

DR - Direct repeats

DRC - Dynein regulation complex

DSB - Double strand breaks

DSBR - Double strand break repair

FPS - Frames per seconds

Hpf - Hours post fertilization

HR - Homologous recombination

HSVMA - High-speed video microscopy analysis

IDA - Inner dynein arms

IFT - Intraflagellar transport

Indels - Insertions or deletions

KV - Kupffer’s vesicle

LB - Luria broth

Mg-ATP - Magnesium adenosine triphosphate

MTBC - *Mycobacterium tuberculosis* complex

NHEJ - Non-homologous end joining.

nNo - Nitric oxide assessments

ODA - Outer dynein arms

PAGE - Polyacrylamide gel electrophoresis

PAM - Protospacer adjacent motif

PCD - Primary ciliary dyskinesia

PCR - Polymerase chain reaction

PKD - Polycystic Kidney Disease

RNA - Ribonucleic acid

RPM - Rotations per minute

RS - Radial spoke

Rsph1 - Radial spoke head protein 1 homolog

Rsph4a - Radial spoke head protein 4 homolog A

Rsph9 - Radial spoke head protein 9 homolog

SDSA - Synthesis depended strand annealing

SgRNA - Short guide RNA

SsDNA - Single strand DNA

SsRNA - Single strand RNA

TALEN - Transcription activator-like effectors nucleases

TEM - Transmission electron microscopy

TracRNA - Trans-activating crRNA

ZFN - Zinc finger nuclease

1. Introduction

1.1 Origin of CRISPR

The unveiling of the fundamental elements CRISPR started early as the 1980 with the discovery of DNA repeats with dyad symmetry by a Japanese research group (Mojica and Montoliu, 2016).These DNA repeats would later become known by, what today is named as, Clustered regularly interspaced short palindromic repeats or CRISPR for short, but at the time researchers could not see the relevance of these repeated clusters, due to lack of homology with other sequences (Marraffini, 2015). Since then, multiple DNA repeats were discovered in various organisms, some of them with close resemblance. This permitted a compressive understanding of the CRISPR loci in bacteria and in archaea (Mojica and Montoliu, 2016). Afterwards, the discovery of interspaced direct repeats (DR) in Mycobacterium tuberculosis complex (MTBC) allowed scientists to strain typing MTBC with ease. Since, DNA sequences between the direct repeats, classified as spacers, showed variability from strain to strain (Hermans et al., 1991). With the increase of the genome database, CRISPR was established as common loci in bacteria and in archaea (Mojica et al., 2000). This was followed by the discovery of small RNAs molecules that are directly transcribed from the CRISPR loci and by the discovery of the Cas proteins (Doudna and Charpentier, 2014). A family of genes linked with the CRISPR that are responsible for chemical reactions that involve nucleic acids. These finding, coupled with the discovery that some spacers contained sequences from phages and plasmids and that the higher the number of spares present in bacteria fewer were the phage that could infect them, suggested that CRISPR associated with Cas proteins were a protection mechanism against phages (Barrangou et al., 2007). This promptly started the pursuit to better understand this defense mechanism.

1.1.1 CRISPR-Cas system involved in bacterial immunity

With several key discoveries suggesting the role of CRISPR in bacterial immunity (Mojica and Montoliu, 2016). The speculation was that CRISPR could work in a similar manner to eukaryotic interference DNA (Makarova et al., 2006). The current understanding is that CRISPR works as a defense mechanism that stores genetic elements of invading phages or plasmid transfers (Mojica et al., 2005). When the cell is attacked, it keeps a record of the genetic elements of that particular phage or plasmid. These elements are integrated into the host in the CRISPR loci forming new spacers. At this point the mechanism of autoimmunity, is capable of distinguishing the invader DNA from the cell own DNA. A failure in this mechanism can lead to an autoimmune response which causes cell death (Jiang and Doudna, 2017). This can be considered the first phase of CRISPR, the adaptation phase or spacer acquisition phase. The next phase consists in the elimination of the foreign DNA. To do that, the CRISPR array is transcribed producing short RNAs that consist in one spacer sequence referring to the foreign DNA. These SgRNAs are then used by the Cas endonucleases to find and cleave the foreign DNAs, see Figure 1.1 (Marraffini, 2015).

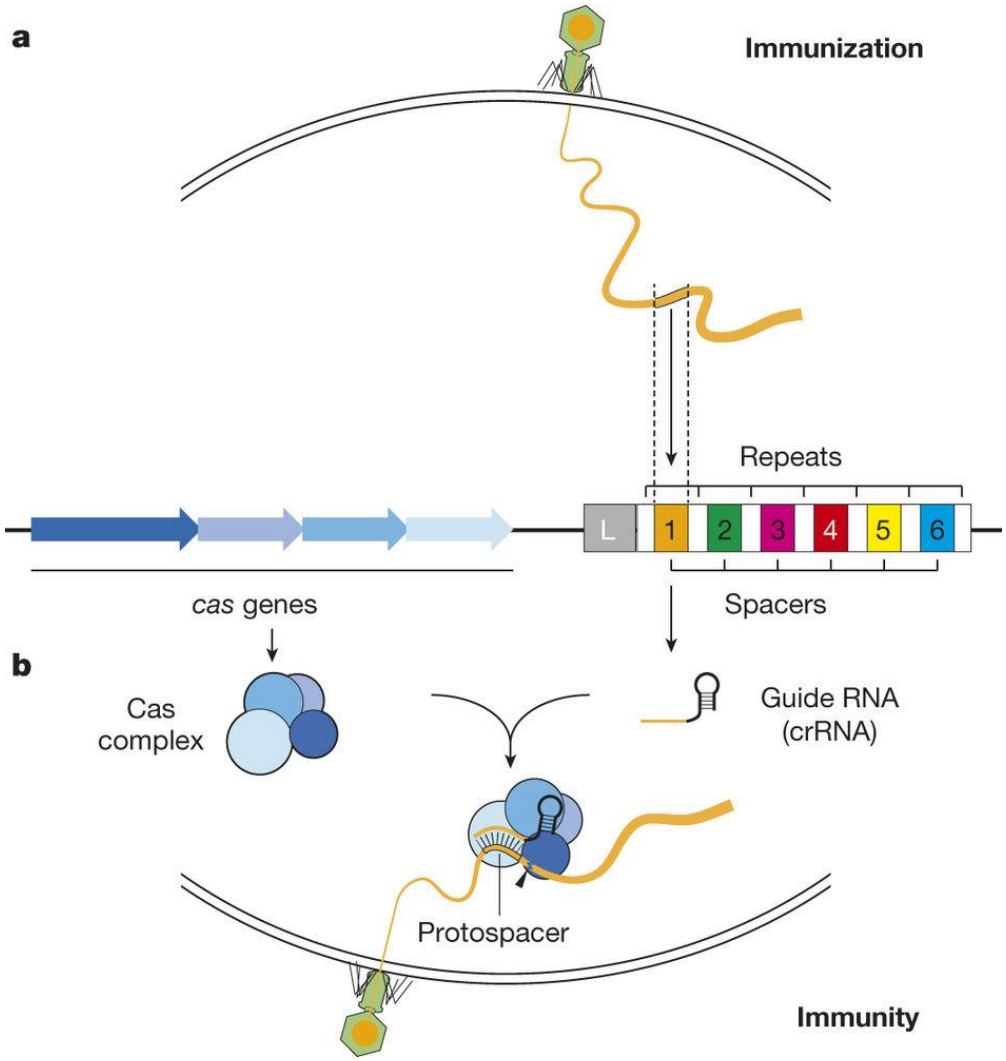

Figure 1.1. CRISPR immunization schematics. (a) infection from phage (b) inner working of the CRISPR as a defense mechanisms. Image and legend adapted from (Marraffini, 2015).

1.1.2 CRISPR-Cas systems classification

The CRISPR system can be classified as type I, II and III (see Figure 1.2). They all have the same molecular mechanism of crRNA guided nucleases, but differ in the biogenesis of crRNAs and the targeting requirements. The crRNA is a small RNA transcribed from the CRISPR loci that contains the same sequence (spacer) that complements the sequence from the foreign DNA and directs the nuclease to that foreign DNA (Jiang and Doudna, 2017). The type I CRISPR-Cas is regulated by the Cas3 nuclease and Cascade complex (see Figure 1.2, a). When the full array of CRISPR is transcribed a repeat-specific endoribonuclease, called Cas6e, cleaves the precursor crRNA (Brouns et al., 2008). This process forms a short crRNA. The crRNA remains associated with cascade and helps this complex locate the target DNA complementary sequence. Another subunit, Cas8, recognizes a short sequence motif located upstream and in close proximity with the target DNA (Sashital et al., 2012). This complementary sequence is known as a protospacer adjacent motif (PAM). After PAM recognition, the

cascade complex recruits Cas3 that induces double stranded breaks (DSB) in the DNA leading to the foreign DNA degradation.

Type II CRISPR-Cas system is simpler than type I and III, only needing Cas9 protein to achieve a DSB in the presence of an existent spacer (Sapranauskas et al., 2011). Although, this system only requires one protein, it needs two types of small RNA molecules to achieve immunity instead. One of the small RNA molecules is a trans-encoded crRNA (tracrRNA), and the other one the crRNA. The tracrRNA binds to Cas9 and forms a secondary structure that mediates its interaction with Cas9. TracrRNA also has a homology zone with the repeats of the CRISPR loci forming and heteroduplex between tracrRNA and pre-crRNA (Figure 1.2, b)(Deltcheva et al., 2011). The double strand RNA is then cleaved by RNase III resulting in the crRNA. The newly formed complex of crRNA and Cas9, tries to locate the PAM which is located downstream of the target sequence (Deveau et al., 2008). When located the CRISPR type II system provokes a DSB in the PAM sequence with the help of two nuclease domains (HNH and RuvC[45]) (Sapranauskas et al., 2011).

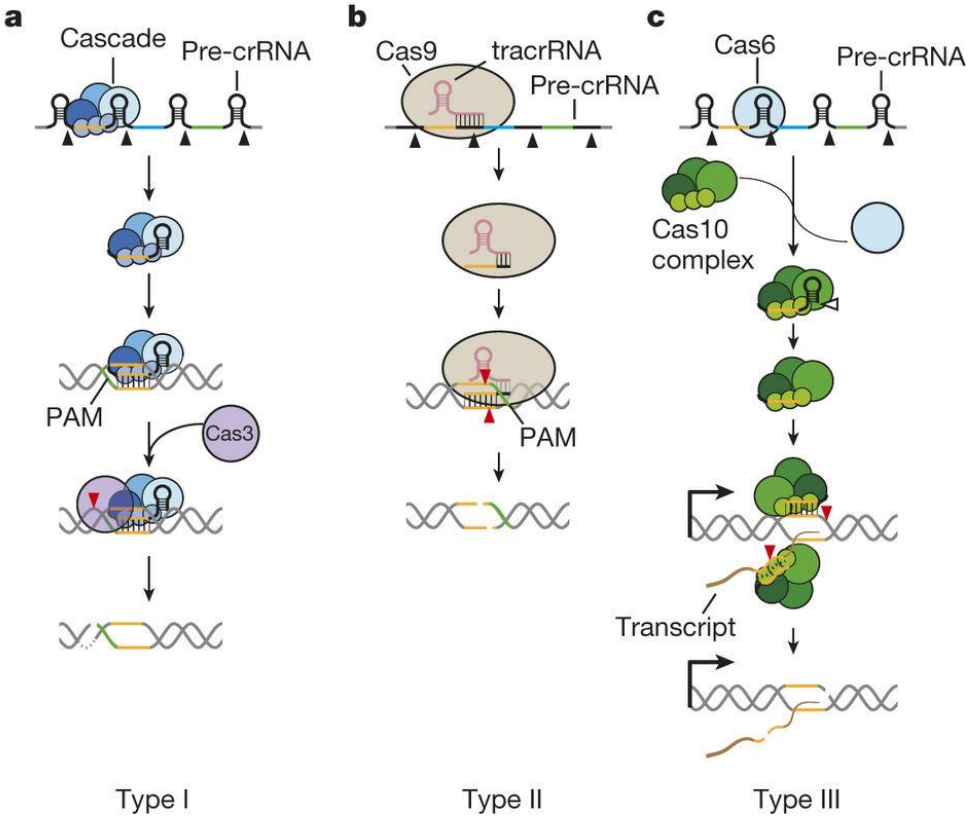

Figure 1.2. Representation of CRISPR different systems. (a) type I system. (b) type II system. (c) type III system. Image and legend adapted from (Marraffini, 2015).

At last, type III CRISPR system (Figure 1.2, c), utilizes Cas6, a repeat specific nuclease to cleave the pre-crRNA. After cleavage, the pre-crRNA becomes crRNA with 8 nucleotides in the 5' end of the repeat sequence as a result of the Cas6 cleavage (Carte et al., 2008). This sequence is known as crRNA tag. Afterwards the crRNA is reallocated to Cas10-Csm, a large complex that matures the crRNA by trimming the 3´end in intervals of 6 nucleotides (Hatoum-Aslan et al., 2013). Unlike type I and II CRISPR systems,

which target the foreign DNA relying only on recognition of the DNA sequence, type III requires the transcription of the target DNA and a crRNA complementarity to the transcripts and to the non-template strand of the DNA target (Goldberg et al., 2014). This results in the Cas10 complex cleaving the non-template strand of the protospacer DNA. Another difference between type III and the other two systems is that, to date, the PAM requirement in CRISPR systems does seem to be needed in type III systems (Marraffini, 2015). So, to prevent autoimmunity, type III systems require differential base paring between crRNA tag and the sequences flaking the protospacer. An incomplete match between crRNA tag and sequences flanking the protospacer results in cleavage and a complete match prevents DNA targeting within the cell (Samai et al., 2015).

1.1.3 Homologous recombination (HR) vs Nonhomologous end joining (NHEJ)

The double strand breaks (DSB) leave the cell with two possible DNA repair strategies, the homologous recombination and the non-homologous end joining (Lieber, 2010). In the absence of a template for the damaged zone, the cell DNA repair mechanism will activate NHEJ. The NHEJ mechanism results from the protein KU binding to each DNA end. The Ku protein serves as tool belt and recruits nucleases (Artemis DNA-PKcs), polymerases (μ and λ) and ligase (XLF XRCC4 DNA ligase IV) to form a complex which then reconnects the DNA (Lieber, 2008). This type of mechanism leads to errors in the repair process, which results in deletions or insertions or even substitutions. Consequently, these errors can cause mutations and disruption of gene function. This approach is very useful when the goal is to study gene function, since it is fairly easy to cause a gene knockout or knockdown. On the other hand, with the presence of a repair template the cell repair mechanism resorts to HR. The DNA repair through HR can be done by two different pathways such as synthesis depended strand annealing (SDSA) or double strand break repair (DSBR) (San Filippo et al., 2008). In the SDSA pathway, when a DSB occurs, the 3' ends of the DNA undergoes nuclease degradation and becomes a single strand overhang, this allows the HR machinery to search the homologous strand in the partner chromosome, when homology is found a displacement-loop (D-loop) is formed between the invading strand and the complementary strand and DNA synthesis begins using the complementary strand as the template (Li and Heyer, 2008). The D-loop is then disassociated and the newly synthesized DNA strand is captured by the other 3' end of the invading DNA forming heteroduplexes and a gap filing DNA synthesis ensues (San Filippo et al., 2008). In DSBR, the initial part of the DNA repair is the same, a ssDNA 3' end finds a homology zone creates a D-loop and starts to elongate. However, in DSBR, the second DSB end can also search for a homology zone resulting in an intermediate state with two holiday junctions. These holiday junctions are an DNA intermediate shaped like a cruciform that are produced when there is a mutual strand exchange between two double strand DNAs, result in a final reparation with DNA crossovers (Sharples, 2001).

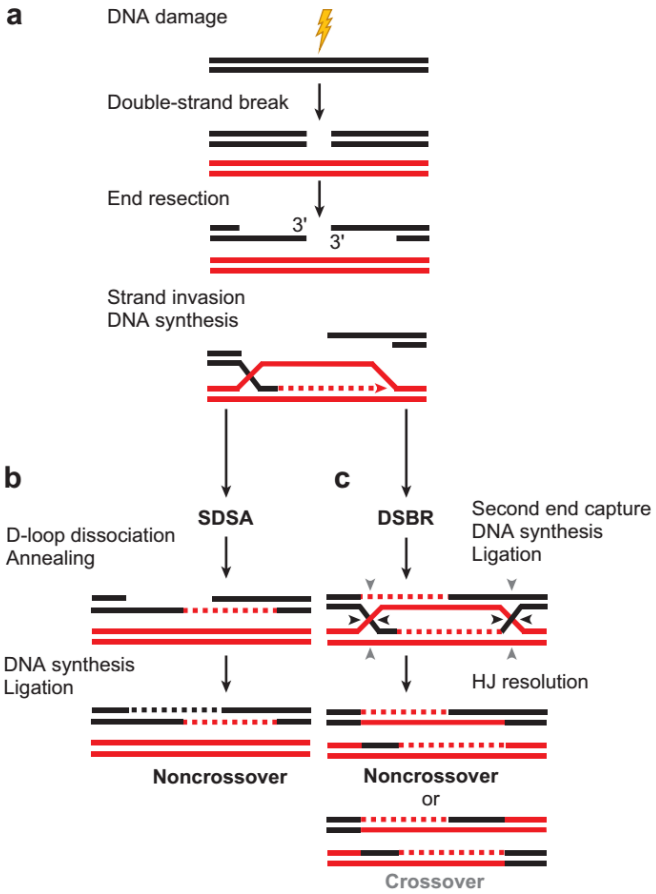

Figure 1.3. Representation of both possible pathway of homologous recombination. (a) a double strand break occurs in the DNA. (b) synthesis-depended strand annealing pathway. (c) double strand break repair pathway. Image and legend adapted from (San Filippo et al., 2008).

1.1.4 CRISPR-Cas9 as a genetic tool

The appeal of using CRISPR-Cas9 type II system as genetic tool is due to the simplicity of the mechanism especially when compared with zinc finger nuclease (ZFN) and transcription activator-like effectors nucleases (TALEN). Although, they all stimulate DNA repair systems at a specific target in the genome (Barrangou, 2013), CRISPR-Cas9 presents a much easier and more convenient solution for gene editing. Both ZFNs and TALENs use protein to achieve homology with the target DNA. In case of ZFNs these proteins are completely synthetic, while TALEN proteins are derived from existing proteins from another organism (Josa et al., 2017). Using both tools can be a tedious and long task and is prone to mistakes. Although TALENs are easier to use, since there is a larger data base with the necessary intermediate plasmids, giving the researchers the flexibility to choose the protein with homology with the target DNA. In contrast, the use of ZFNs is largely limited, since ZFNs are only available commercially, which removes some of the autonomy from the investigations (Josa et al., 2017). These factors along with the ease of customization, allows researchers to target different sequences which makes CRISP-

Cas9 the elected system. By only needing to change the 20 nucleotides of the guide sequence, allows researchers to virtually target any part of the DNA (Ran et al., 2013). Furthermore, a predictable cleavage pattern and the high efficiency made CRISPR a very compelling alternative (Jinek et al., 2012; Hoshijima et al., 2016). The only limitation in using CRISPR-Cas9 is the PAM. Each Cas9 ortholog as a different PAM sequence, which can limit the targeting range (Ran et al., 2013). Also, off target mutants can also occur.

This plasticity of CRISPR-Cas9 could allow scientist to target the genome of any species, resulting in a range of possibilities. From gene knockout, to study of gene function, to gene editing for creation of transgenic organisms or even for genetic therapy. An interesting approach is to use CRISPR-Cas9 as tool to create mutations in animal models that mimic diseases present in humans. This would allow a better understating of diseases that affect humans. Such is the case of ciliopathies, a group of diseases characterized by the malfunction of the cilia, like primary ciliary dyskinesia (PCD). PCD has been linked to a number of genes (Verhulst et al., 2007; Castleman et al., 2008; Antony et al., 2013; Lai et al., 2016). A better understating of the gene association with cilia motility or assembly, would help characterize PCD.

1.2 Cilia

Cilia or flagella, are hair-like structures that protrude from the cell surface in organisms that can range from single cell eukaryotes to more complex organisms and are almost ubiquitously present in all cells across vertebrates (Fliegauf et al., 2007). These structures were highly preserved throughout evolution, which indicates the importance of these organelles in the development and maintenance of cells and organisms life. Cilia have been associated with a variety of important roles depending on their subtype. Cilia can be motile or not. Non-motile cilia, also known as primary cilia, functions as the cells antenna's, displaying several receptors. Primary cilia malfunction can generate disease like Polycystic Kidney Disease (PKD), Bardet−Biedl Syndrome (BBS), Alström Syndrome (ALMS) (Badano et al., 2006).The roles of motile cilia include motility of single cell organisms, generating fluid flow and sensing mechanical or chemical cues (Ishikawa and Marshall, 2017). These roles can be compromised if there are any defects in the cilia assembly or in its components. Impairment in the molecular complexes that are needed to cilia structure, functions and maintenance, can lead to ciliopathies. Defects in motile cilia can lead to a disease known as primary ciliary dyskinesia (PCD). This pleotropic disorder can present phenotypes such as upper respiratory tract infections, male infertility and left-right body asymmetry defects (Kobayashi and Takeda, 2012)

1.2.1 Cilia classification

Cilia and flagella are fundamentally equal when compared structurally and functionally, despite having different designations. Even so, cilia can differ depending on the function they perform. Different specializations of cilia have impact in their structure and regulation. This impact allows the classification of cilia in two classes, the primary cilia or motile cilia.

Primary cilia, typically appear in the cell surface of several cell types including stem, epithelial, endothelial connective tissue, muscle cells and neurons. Primary cilia are single, normally non-motile organelles that originate from the cell surface of most cells. They are formed by a “9+0” conformation. On the other hand, motile cilia have a “9+2” conformation. The 9 refers to the number of peripheral doublets present in the ciliary axoneme while the 0 or 2 refers to presence or absence of the central pair. Typically, it was thought that primary cilia immobility was due to the lack of central pair, however studies demonstrate that motile cilia can have a “9+0” and can still be motile (Sobkowicz et al., 1995; Satir and Christensen, 2007). So, the lack of mobility of the primary cilia is not due to the absence the central pair, but because the outer and inner dynein arms as well as the radial spokes are missing (Fisch and Dupuis-Williams, 2011; Kobayashi and Takeda, 2012).

Since, most primary cilia are immotile it is thought that they have a major role in cell signaling function due to the presence of several receptors in the ciliary membrane, like ion channels and transporter proteins. In addition, signaling effectors were found in the basal body and along the cilium (Singla, 2006). Primary cilia are often compared to an antenna, as the presence of receptors allows the cilium to establish signaling in a concentrated microenvironment (Hilgendorf et al., 2016).

The ability to signal is very important since signaling in the cilium coordinates key processes during development and in tissue homeostasis, including cell migration, differentiation and/or re-entry into the cell cycle, specification of the plane of cell division, and apoptosis. The primary cilia can also respond to mechanical stimulation (bending of the cilium by the fluid forces) or chemosensation (recognition of ligands, growth factors, hormones or morphogens) (Singla and Reiter, 2006). Some sensory organs have specialized cilia capable of sensing light and detect odorants (Ishikawa and Marshall, 2017).

In contrast, the motile cilia are less widespread being present only in a few cell types like sperm, epithelia of the upper and lower respiratory tract, oviducts and ependymal cells in the ventricles of the brain. Being that this type of cilia are motile they play an integral role in locomotion, in case of the sperm, and in making fluids flow (Ishikawa and Marshall, 2017). Motile cilia are normally found in multiciliated cells at high density beating in a synchronized fashion. This synchronized beating is responsible for mucus clearing in the airways or in aiding passage of cerebrospinal fluid within the brain and spinal cord. In the case of motile monocilia cells such as the sperm, only one long cilium generates thrust. This notion that motile cilia were only capable of generating fluid motion or cell locomotion was shattered, when it was discovered that motile cilia also have the capability of perceiving osmotic forces, bitter taste, stress, fluid flow and sex hormones (Jain et al., 2012).

1.2.2 Cilia ultra-structure

The cilium is a protrusion from the cell membrane, consisting in a cylindrical structure called the axoneme. All axonemes are comprised of nine outer doublets and a central pair in case of motile cilia. Primary cilia, lack the central pair. So, immotile cilia are usually classified as “9+0” and motile cilia as “9+2”. The outer doubles are microtubules that extend from the basal body of the cilia. One complete microtubule extends from the basal body (A tubule) and connects with and incomplete microtubule (B tubule) (Ishikawa and Marshall, 2017). These microtubules are often subjected to tubulin post translation modifications such as acetylation, glutamylation, and glycytion, these modification are important, since the axoneme is the core of the cilium and also responsible for the transportation of ciliary proteins, and these modification were implicated in axoneme stability, assembly and even motility of the cilia (Ikegami and Setou, 2010). These peripheral microtubules, in the case of motile cilia, are associated with multiple accessory proteins like radial spokes, dynein arms and nexin links. The nexin links connects the adjacent microtubules to each other whereas the radial spokes connect the outer microtubules with the central pair (see Figure 1.4) (Kobayashi and Takeda, 2012).

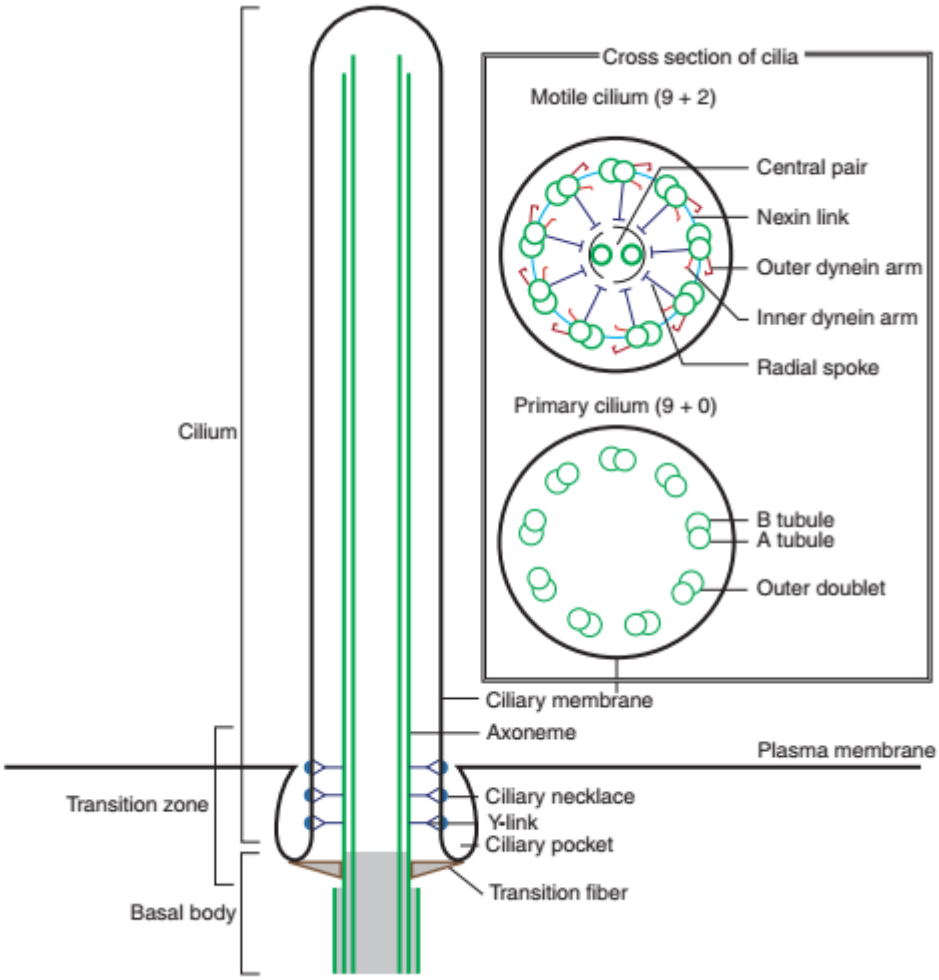

Figure 1.4. The architecture of cilia. Schematic, foreshortened drawing of a longitudinal section of the primary cilium. The inset shows cross sections of motile and primary cilia. Image and legend from (Ishikawa and Marshall 2017).

The dyneins are large protein complexes encompassing several chains, ranging from light (8-55 kDa) to intermediate (45-110kDa) to heavy (400-500kDa) and are the force behind the ciliary movement. The outer dynein arms (ODAs) are positioned and located closer to the cilium membrane and further from the central pair. In contrast, the inner dynein arms (IDAs) are located closer to the central apparatus and further form the cilium membrane (Kobayashi and Takeda, 2012). The dynein arms can be classified according to the number of heavy chain motors that they contain. Dyneins with only one motor unit form the first class. These motors form a subset of inner dynein arms that arrange in a complex manner along the axonemal length or even with specific outer doubles. The second class of dyneins include both the inner and outer arm dyneins and are composted by two motors that associate together via their amino terminal region. These motors are closely related to the motors that power the retrograde intraflagellar transport (IFT) (King, 2016).The region between the cilium and the basal body is named transition zone. In this zone, there are transition fibers that anchor the mother centriole to the plasmatic membrane. Above this region, Y link bridges connect the axoneme microtubules to the cilium membrane (Ishikawa and Marshall, 2017).

1.2.3 Ciliogenesis

Ciliogenesis is a highly complex process, involving several steps that are in coordination with the cell cycle progression and differentiation. To start the cilium assembling, the cells must exit the mitotic cycle in order to free the centrioles for axoneme nucleation. There is a link between ciliogenesis and cell division, since improper cell division can lead to an abnormal ciliogenesis (Prachee Avasthia, 2012). For ciliogenesis to occur various components need to be dislocated from the Golgi complex and cytoplasm to the close vicinity of the basal body. The mother centriole acquires an array of distal and subdistal appendages (Anderson, 1972) and forms the basal body. The basal body will then interact with a post Golgi vesicle that upon extension of the microtubules will flatten, envelops the axoneme giving rise to the cilia membrane (Sorokin, 1962; Lu et al., 2015). This basal body will then dock into a actin-rich cortex and fuses with the membrane (Ishikawa and Marshall, 2011). Afterward, the cilium starts to protrude from under the membrane, due to the outgrown of the axonemal microtubules. The manner in which this basal body is established, dictates the alignment of the emerging cilia. Afterward, the outer doublets start to form in the transition zone of the cilium and all the outer doublets assembly occurs in the distal part of the cilium. Since the cilium cannot synthesize any protein by itself it recurs to intraflagellar transport (IFT), to produce an efficient trafficking of proteins along the cilium. IFT is the bidirectional transport of proteins along the axoneme from cilium base to the tip and vice versa (Vincensini et al., 2011). The bidirectional transport can be characterized as anterograde movement, when the transport of particles is made in direction of the cilium tip, or retrograde movement if the transport is made from the tip to the cilia base. The anterograde movement is mediated by kinesins of the kinesin2 family while the retrograde movement is mediated by dyneins of the cytoplasmic dynein 2 family (Figure 1.5). IFT is necessary for cilia growth and maintenance (Ishikawa and Marshall, 2017).

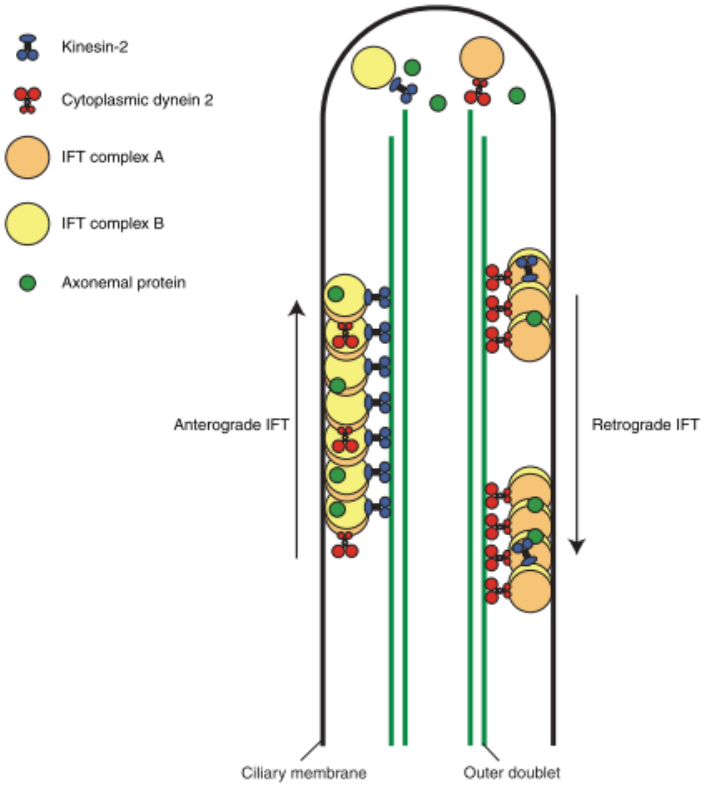

Figure 1.5. Intraflagellar transport. The anterograde intraflagellar transport (IFT) motor kinesin-2 transports IFT complexes A and B, axonemal proteins, and cytoplasmic dynein 2 to the tip of a cilium. At the tip of the cilium, anterograde IFT "trains" release axonemal proteins and rearrange their conformation for retrograde IFT. Cytoplasmic dynein 2 transports retrograde IFT trains to the cell body. Image and legend from (Ishikawa and Marshall 2017).

1.2.4 Dynein based motility

The motility of the cilia is dependent on the dynein arms (IDAs and ODAs) that are formed in the outer doublets. Dyneins are huge molecular motors (1-2 MDa) that can generate force (King, 2000). Although IDAs and ODAs are homologous structures and both contribute for motility, their molecular composition and arrangement with the axoneme is completely different. Morphologically there is only one form of ODAs while IDAs have two, one with two heads and other with three (Goodenough, 1985). The outer dynein arms are spaced in the microtubule 24 nm apart, while the triplets dyad heads of the inner arm are spaced 96 nm apart along the axoneme (Kamiya, 1991). In *Chlamydomonas*, analyses of ODA and IDA mutants demonstrate that, ODAs are more important for high frequency beating while IDAs are necessary for proper formation of ciliary waveforms (Yagi et al., 2005).

For proper cilia beat function the dynein motors must be extremity well regulated, to allow a wave of activity to be propagated from the basal body to the tip of the cilia. For that, opposing hemispheres should be turn on and off alternately, allowing the cilia to bend (King, 2000). This is thought to be regulated by the interaction between inner dynein arms and the radial spokes, since there is a strong suggestion, that the radial spoke regulates the inner dynein motors via phosphorylation. (Zhu et al., 2017). The core of ciliary movements is the sliding of the doublets of microtubules relative to each other

due to the force generated by dynein motors when in presence of Mg-ATP. The sliding of the microtubules results in a bend of the axoneme because the basal body anchors the cilium at the base and the nexin links connect the doublets along the axoneme (Lindemann and Lesich, 2010).

1.3 Ciliopathies

Throughout the human body, most cells contain cilia. These include the eye, the trachea, the kidney, the reproductive system, the intestines, the heart and other organs. In each cell, each cilium has a role to fulfill, and impairment in that role can lead to severe consequences. Most contain a single non-motile cilium which serves as receptor to capture information from the local environment. Because of this signaling role, there is an increased appreciation of the cilium function in developmental processes and homeostasis in vertebrates. The role of motile cilia has also been recognized and their dysfunction has major manifestations in mammals such as, respiratory dysfunction, reproductive sterility and hydrocephalus, see Figure 1.6 (Badano et al., 2006).

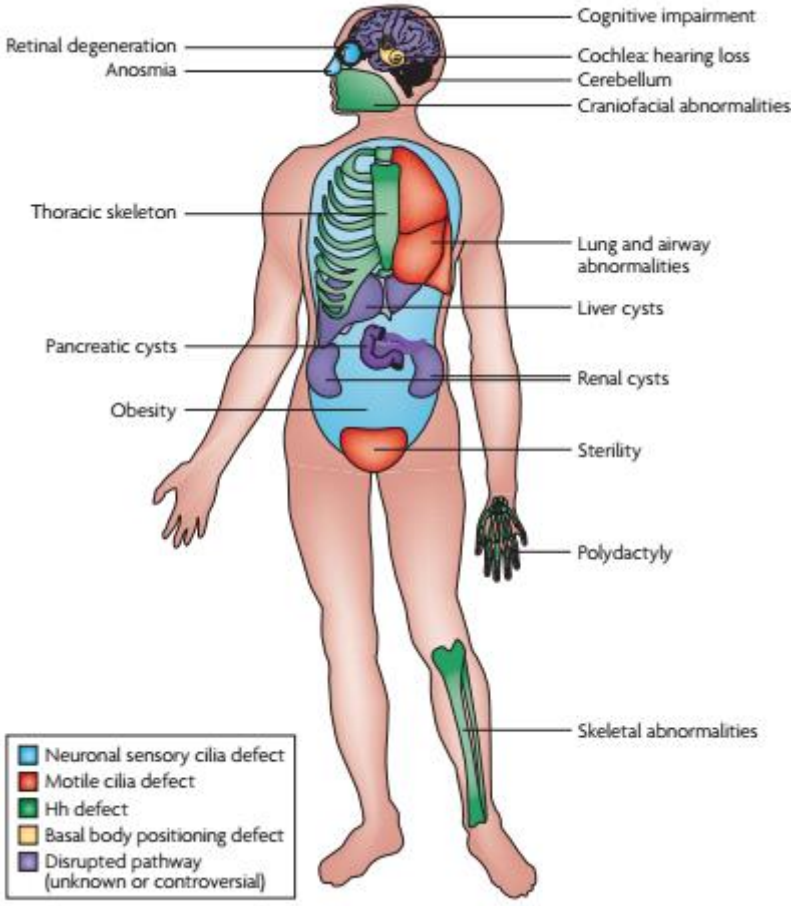

Figure 1.6. Organs that can suffer from problems due to ciliopathies throughout the human body. Diseases that are caused by ciliary defects and hedgehog defect throughout the human body. Some defects are attribute to hg such as skeletal abnormalities, other are exclusively to cilia related defects like infertility in male and females. Image adapted from (Goetz and Anderson 2010).

Ciliopathies are pleotropic disorders caused by mutations in a great number of gene that are necessary for cilium assembly and maintenance. These genes code for proteins that interact with various protein complexes that are present in the cilium, basal body, centrosome and others (Hildebrandt *et al*.,2011). A failure in any of these processes can lead to disease such as, retinitis pigmentosa, polycystic kidney disease (PKD), nephronophthisis, Bardet-Biedl syndrome (BBS), primary ciliary dyskinesia (PCD), various skeletal dysplasias and even cancer (Hildebrandt et al., 2011; Horani and Ferkol, 2016). In case of PCD, around 50% of patients also present *situs inversus*, a total reversal of the internal organs and 6% may present heterotaxia, a partial reversal of organs (Kennedy et al., 2007).

1.3.1 Primary ciliary dyskinesia (PCD)

Primary ciliary dyskinesia or PCD is a term used to describe patients who suffer from a primary defect in cilia structure and function. PCD is usually an autosomal recessive disease with an incidence of 1 in 10,000 people, making it a rare genetic disorder (Zariwala et al., 2011). PCD true prevalence is unknown due to many patients being misdiagnosed or not diagnosed at all. A study shows that 37% of the patients have more than 20 visits to a medical professional, with problems related with PCD, before being redirected to a proper PCD diagnostic unit (Behan et al., 2016).

PCD patients have impaired mucociliary clearance, which is an important defense mechanism for removing bacteria and debris from the airways. This leads to paranasal sinuses and causes a frequent chronic infections of the upper and lower respiratory airways (Rubbo and Lucas, 2017). PCD patients can also present signs of infertility or low fertility, due to reduced sperm motility or, in case of women, defects in the fimbriae of fallopian (Behan et al., 2016). Around 50% of patients suffer from laterality defects like *situs inversus* (Chodhari et al., 2004) or from *situs ambiguous* which in some cases can be associated with congenital heart failure (Olivier et al., 2014). Sometime patients can present a different array of a combinations of symptoms and these can vary during the patient life time.

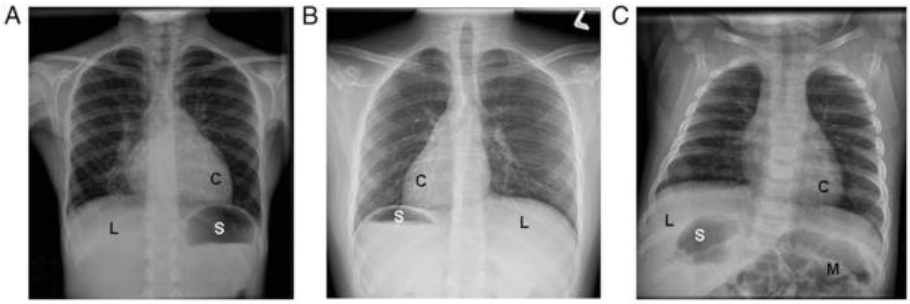

Figure 1.7. Examples of laterality defects on radiology imaging in various situs groups in the study population. A, A participant with situs solitus, or normal organ arrangement, with left cardiac apex, left sided stomach bubble, and right-sided liver. B, A patient with situs inversus totalis, or mirror image organ arrangement, with right sided cardiac apex, right sided stomach bubble, and left sided liver. C, A patient with situs ambiguous with left sided cardiac apex, right-sided stomach bubble, right-sided liver, and intestinal malrotation who also has right sided polysplenia visualized on CT scan. C 5 cardiac apex; L 5 liver; M 5 intestinal malrotation; S 5 stomach. Legend and image adapted from (Olivier et al., 2014).

So far, more than 35 gene have been associated with PCD patients (Kuehni and Lucas, 2017). Defects in outer dynein arms and in inner dynein arms are the most common type of ultrastructure defects encountered, being that ODAs defects can account for 18% to 30% of the reported cases (Zariwala et al., 2011). Defects can range from absent or reduce outer dynein arms or inner dynein arms, or both in conjunction, absent radial spokes, absent central pair with transposition of peripheral microtubules doublets to the center, peripheral defect, complete ciliary aplasia and defects in cilia orientation (Chodhari et al., 2004).

A gene like *dnah5*, which encodes a heavy chain protein of the ODA, already has been associated with mutations that lead to ODA defects. A premature truncation results in an absent set of ODAs while, splice site mutations results in shorten ODAs, but not absent (Verhulst et al. 2007). Other genes like *ccdc39* and *ccdc40* also have been associated with PCD, these genes encode proteins involved in dynein regulatory complex (DRC), which interacts with the DRC subunits. Is also possible that *ccdc39* and *ccdc40* have roles in cytoplasmic pre-assembly of axonemal proteins or axonemal targeting and transport of the axonemal components (Zariwala et al., 2011). Patients with mutation in these genes have cilia with a very stiff movement and poor amplitude.

In PCD diagnostics there is no “gold standard “, instead the use of a combination of PCD-specific tests is a requirement for proper diagnosis. The diagnosis testing for PCD should be based in clinical symptoms, nasal nitric oxide assessments (nNO), high-speed video microscopy analysis (HSVMA), transmission electron microscopy (TEM) and genotyping (Lucas et al. 2016). The use of TEM was once considered the “gold standard” in PCD diagnostics. However, TEM became a less effective diagnostic tool when it was found out that 15-20% of cases of PCD have a normal ultrastructure (Raidt et al. 2014). In alternative HSVMA can be used as a first line of diagnostics, since it is the only test to directly analyzes ciliary frequency and beat pattern. Recent studies indicating that an association between CBF, ultrastructure defects analyses and genotyping, would help to consolidate HSVMA as a good tool for PCD diagnostics. Defects in ODAs and IDAs present an immotile cilia phenotype, while defects in only ODAs, like *dnah5*, defects are associated with reduced movement and regions of static cilia (Raidt et al. 2014). Although, HSVMA is still dependent on having an expert eye for an accurate diagnose. Other methods like genotyping and immofluorescence (IF) of ciliary proteins can be used (Lucas et al., 2017). International networks like the ongoing Beat-PCD COST European action are multi-country projects that aim to standardize the PCD diagnostic, clinical care, epidemiology and the fundamental scientific knowledge on PCD.

1.4 Genes of interest for this Master thesis

Several genes so far have been associated with PCD, so in order to better characterize the mechanisms behind the disease a group of genes were selected, to try to study the effects of their absence in zebrafish. The genes selected were *dnah7*, a gene encoding for an inner dynein arms responsible for motion in the axoneme and *rsph4a*, a gene responsible for coding the radial spoke head of cilia, which

is also responsible for the regulation of inner dynein arms. The MO against *ccdc40* gene was later considered as a good alternative for replacing the toxic *dnah7* MO for cilia movement disruption.

1.4.1 *Dnah7*

Dynein axonemal heavy chain 7 or *dnah7* is gene responsible for cilia movement and has been identified has a component of the inner dynein arms of ciliary axonemes (Zhang et al. 2002). *Dnah7* seems to be a major player in cilia beat, since when it is not assembled it results in a ciliary dysfunction (Prachee Avasthia 2012). To date no PCD patient has been associated with *dnah7* mutations. Although it was thought to be found in a PCD patient, it was later revealed that there was no mutation in *dnah7*, only a polymorphism and that the likely cause of the phenotype was related to the assembly or transport factor of *dnah7* and not *dnah7* itself (Zhang et al. 2002). Furthermore, other genes like *dnah5* and *dnah11*, which also encode for dynein heavy chains, have been linked to PCD patients (Zariwala et al., 2011). Additionally, studies with *dnah7* morpholino in zebrafish, showed a total absence of CBF in the left-right organizer, originating a great number of left-right defects (Sampaio et al., 2014). In zebrafish, *dnah7* is a gene located in chromosome 9 that codes for 3 transcripts (splice variants) and has 51 orthologues and 11 paralogues. *Dnah7-202* is the larger transcript, comprised by 12.260 bp and 4001 amino acids. *Dnah7-201* is the second biggest composed by 3086 bp and 584 amino acids. The smaller transcript in *dnah7*-203 has 557 bp and 165 amino acids.

1.4.2 *Rsph4a*

Rsph4a is a gene that encodes a protein of the axonemal radial spoke head, hence the name. The interaction between radial spokes and the central apparatus of the axoneme with “9+2” configuration has fascinated many people (Zhu et al., 2017). The radial spoke is an essential component of “9+2” axoneme of motile cilia. The central pair interacts with the radial spokes to activate sub-sets of dynein arms and thus controlling cilia waveform (Porter and Sale, 2000). Humans and *Chlamydomonas reinhardtii* missing part or complete radial spoke heads present paralyzed cilia or cilia with an abnormal beating pattern (Yang, 2006; Castleman et al., 2008). This gene is located in chromosome 5 of zebrafish and has only one transcript with 1775 bp and 524 amino acids with 79 orthologues.

1.4.3 *Ccdc40*

The gene *ccdc40* or coiled-coil domain containing 40 is responsible for an evolutionary conserved role in the assembly of motile cilia and establishment of the left-right axis. It regulates the assembly of inner dynein arms and DRC, which are necessary for cilia movement and control (Sui et al., 2016). A mutation in *ccdc40* leads to structure defects such as duplication or misplacement of microtubule doublets, missing or reduced number of IDAs, and affected radial spokes and nexin links (Sugrue and Zohn, 2017). Overall, *ccdc40* defects create a disorganization on the axoneme and leads to PCD (Antony et al., 2013). *Ccdc40* is composed by two transcripts, one larger (*ccdc40-202*) and a smaller one (*ccdc40-201*). The

larger transcript encodes for a protein with 941 amino acids, from 3370 bp and the smaller one is non-coding. This gene is located in chromosome 6 of the zebrafish.

In conclusion, we have targeted genes that encode for some important component within the motile cilium, either by being part of inner dynein arm or the radial spoke or being an essential assembly factor for dynein arms.

1.5 Zebrafish as an animal model

Zebrafish or *Danio rerio* is a small vertebrate and is used as an animal model due to its great practicality and versatility. *Danio rerio* is a good model for genetic diseases and other type of biological processes like tissue regeneration, infectious diseases, cancer metastases and pharmacology studies (Baxendale et al., 2017). Aside this versatility, *Danio rerio* is also very practical and easy to maintain. A full grown zebrafish can reach 3 cm and can be easily maintained in an aquarium with other zebrafish, reducing the overall space needed for zebrafish rearing. Breeding zebrafish, is fairly easy, with one female capable of laying hundreds off eggs in each clutch (100-200 eggs), resulting in huge number of progeny facilitating processes such as screening for a rare mutation where the incidence rate maybe low. Furthermore, larva are only a couple millimeters in size and can be pooled together in a petri dish and until 5 days post fertilization (Mushtaq et al., 2013). Other reason behind the attractiveness of zebrafish for research is the rapid development, since embryogenesis is almost complete by 72 hpf and the internal organs are developed and functional and fully mature within 3-4 months (Parng et al., 2002). Aside the rapid development, other advantages are the transparency of the embryos enabling the imaging of internal cells and structures in real time under the microscope. Furthermore, the embryos develop externally, which allow clear visibility of the development stages. Also, zebrafish are relatively cheap to maintain when compared to mammals (Baxendale et al., 2017)

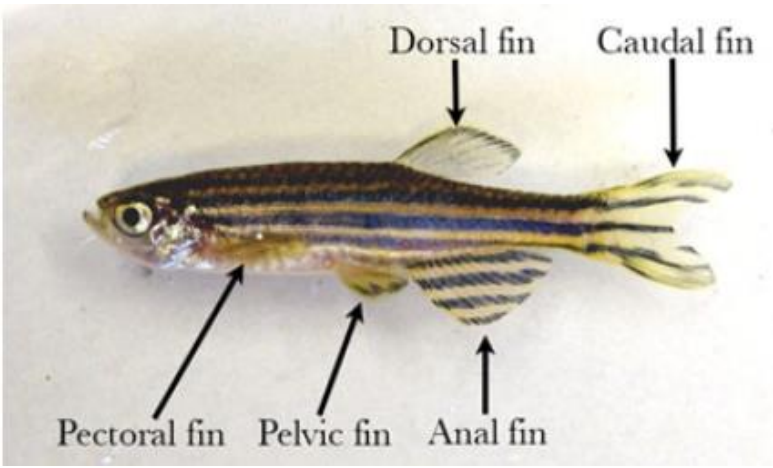

Figure 1.8. Adult zebrafish. Side profile of an adult zebrafish, with the classification of all fin present in a healthy adult zebrafish. Image adapted from (Gupta and Mullins, 2010)**.**

The zebrafish animal model is relativity new when compared with other used animal models, however, despite of not being a mammal there is a large gene conservation between fish and humans.

Approximately 80% of 523 orthologous genes fall in a conserved synteny (Barbazuk et al., 2000). Additionally, zebrafish almost have the same number of chromosomes as human, 25 to 23 respectively. All these characteristics, coupled with advance in genetics which can introduce many human traits in zebrafish (Mushtaq et al., 2013) make a very good argument to use *Danio rerio* as an animal model.

1.6 Project goals

The main objective of this thesis was to create a *Danio rerio* / zebrafish mutant using the recent CRISPR-Cas9 tool. In the process of creating a mutant, a protocol would be established for future use with other genes. For this thesis, the principal target was *dnah7* gene. This gene codes for a dynein heavy chain present in the inner dynein arm of motile cilia. A disruption in this gene was anticipated to cause a phenotype similar to the effect of the *dnah7* morpholino (MO) previously used in the lab. The *dnah7* MO generated static cilia and a randomization of the organs in zebrafish (Sampaio et al., 2014). The mutant should confirm the morpholino effect and test if the observed ciliary dyskinesia was due to any toxicity or to real inner dynein malfunction. A full comparison between the morpholino knockdown and the mutant knockout was predicted to be out of scope of the Master project due to time constrains in growing the correct number of generations.

So, while the F0 generation of the *dnah7* potential mutants were growing, the secondary aim of this thesis was to finish the generation of another cilia motility disease model the, *rsph4a* mutant, also using CRISPR-Cas9 technology. This project was started by a PhD student and was continued in the scope of this thesis. The goal was also to disrupt the cilia beat frequency, for the future study of its implications in organs that have motile cilia for comparison to human mutations in the same gene.

The third goal was to functionally study the impact of the generated mutations or knockdowns on the cilia motility of the motile cilia present in the spinal canal of the zebrafish larvae.

In short, the main objectives were:

1. Establish a CRISPR-Cas9 protocol for future studies

2. Create *dnah7* mutants to validate *dnah7* role in cilia function investigated before in the lab by Sampaio et al. (2014).

3. Create *rsph4* mutants for mimicking human mutations

4. Study the cilia beat frequency of the spinal canal motile cilia from wild type and compare it to *dnah7* and *ccdc40* knockdown larva.

2. Materials and Methods

2.1 Establish a breeding guide

The goal of my thesis was to make a clean and stable zebrafish mutant lines for the genes *dnah7* and *rsph4a* using the new technology CRISPR-Cas9. After injecting the embryos with the designed short guide RNAs and screening for the mutation, the embryos would form the F0 generation or the “Crispant” generation (see Figure 2.1). This generation would be formed by heterozygotes fish, meaning that at least one of the chromosomes would have the desired mutation. Then, after the F0 generation become fully mature, their gametes would have to be collected and screened for mutations in the region of interest. If present, the founder fish were then crossed with a wild type line creating the F1 generation. The F1 generation is a cross between the “Crispants” and wild type fish, this out-cross is made to “clean” the genome from other undesirable mutations created with CRISPR-Cas9 to then hopefully pass along only the desirable one. When fully matured, the gametes from F1 would be collected and once again checked for mutations. If mutations were found, the F1 generation was then in-crossed, to generate 25% of homozygous fish for the mutation. Ideally, these would be grown to adulthood.

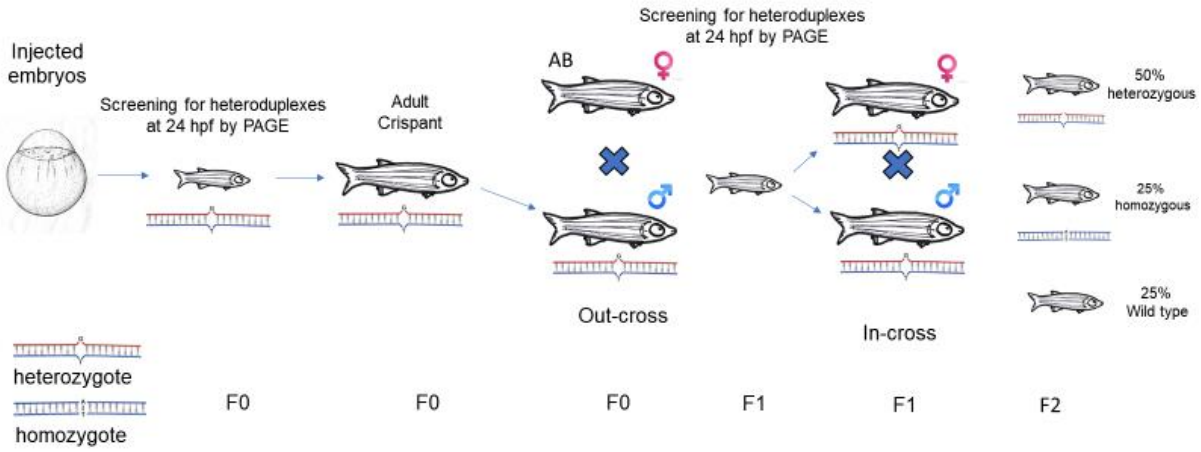

Figure 2.1. Schematics of the breeding process to achieve a clean and stable mutant line. The embryos injected with SgRNAs are screened for heteroduplexes by PAGE. If found they are left to mature for 3 to 4 months. When sexually mature, they are out-crossed with a wild type zebrafish and the progeny originated from this cross is screened for heteroduplexes. If heteroduplexes are found, the fishes are left to sexually mature. If during the previous screening, if a male and a female are found with an interesting mutation, then those fish are in-crossed. The result is a progeny consisted with 50% heterozygous zebrafish for wild type and mutants DNA, 25% homozygous form wild type DNA and 25% homozygous for mutant DNA.

2.2 Choosing the Short-guide RNAs (SgRNAs)

To induce mutations on the target genes, *dnah7 and rsph4a*, multiple short-guide RNAs (SgRNAs) were chosen based on the novel scoring algorithm program from Giraldez Lab (Yale University) that can be found online in www.crisprscan.org. To sketch these SgRNAs, the coding DNA sequence or CDS of each gene was acquired at http://www.ensembl.org/. By using CDS instead of the genomic sequence,

we guarantee that the chosen SgRNA targets the exons. Therefore, ensuring that the indels remains even after the splicing. The SgRNAs were obtained at http://www.crisprscan.org, a sgRNA design web page. This web page grants the ability to see SgRNAs target sites available for a specific CDS. The goal was to create a SgRNA that could disrupt the gene and hopefully create a deletion or an insertion (indels) by non-homologous recombination. The first SgRNA (SgRNA1) for the *dnah7* gene was selected to disrupt the two largest transcripts from the *dnah7* gene (Figure 2.2). This SgRNA targets both transcripts very close to the beginning of each transcript. This way, both transcripts could be affected reducing or eliminating any redundancy between them. For the second SgRNA (SgRNA2), the strategy was to disrupt the ATPase domain of the *dnah7* protein and create a malfunctioning protein. This approach was selected since, the ATPase region from the human *dnah7* gene and the zebrafish *dnah7* gene were very similar, presenting 72% of homology between both sequences (Annex I). The third SgRNA targets the beginning of the first transcript more specifically in the third exon. By targeting closer to transcription start site there is a higher chance of creating a null allele and thus generating an interesting strong phenotype. The *rsph4a* SgRNAs were selected by a PhD student in the lab. The strategy was to target the third exon of *rsph4a*, since it presented 50% homology with the human *rsph4a* and there were known human mutations in this region that we wanted to mimic see Annex II. Three sgRNAs were chosen, but only two were synthesized. Ultimately, all the SgRNAs were selected to generate non-functioning proteins.

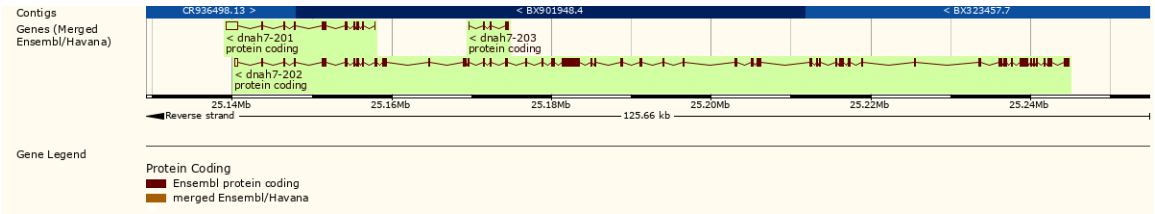

Figure 2.2. Transcripts of zebrafish *dnah7* gene. Number of transcripts that *dnah7* encodes, their location and in relative size to each other. Image obtained at http://www.ensembl.org/Danio_rerio/Gene/Summary?db=core;g =ENSDARG00000060165;r=9:25128793-25254454.

The SgRNAs selected obeyed several parameters to maximize the chance of creating a disruption in the target gene. The first parameter was that the sgRNA had to canonical. For a sgRNA to be canonical, means that the sgRNA is 100% equal to the genomic DNA target. The problem arises from a necessity of the first two base pairs to be “GG”, since the “GG” is needed for the proper transcription of DNA to RNA. Some SgRNAs may not have the “GG” in the first two bases, so the match between the sgRNA and the genomic DNA will not be 100% therefore, being non-canonical. Although, a non-canonical sgRNA can be used, its efficiency may be reduced compared to the counterpart. The second parameter was the score that the sgRNA design web page gave to each sgRNA. The higher the score the more efficient that particular sgRNA would be. The third parameter was the location of the sgRNA, generally all the sgRNA were chosen to target the beginning of the CDS sequence. Aside from the *dnah7* SgRNA1 that was selected to target the ATP region of the gene. The forth parameter used was the number of mismatched that the sgRNA could have in the DNA. All SgRNAs selected had zero mismatches, this

way we can guaranty that the SgRNA doesn't match in other regions of the DNA, therefore, having a specific SgRNA that matches only in the region of interest.

Table 2.1. SgRNAs selected to use in *dnah7* gene disruption.

Target gene	Forward strand	Reverse strand
dnah7 Sg1	TACTCTAAAGCCCATCAT	ATGATGGGCTTTAGAGTA
dnah7 Sg2	CTTGTGGCTGACCAGTT	AACTGGTCAGCCACAAG
dnah7 Sg3	CGCTGGCATGAAGCAAGTCC	GGACTTGCTTCATGCCAGCG

Table 2.2. SgRNAs selected to use in *rsph4a* gene disruption

Target gene	Forward strand	Reverse strand
rsph4a Sg1	CGATTCTGGGGCAAGATTCT	AGAATCTTGCCCCAGAATCG
rsph4a Sg2	GCTCTTGCGGTGTCGATTCT	AGAATCGACACCGCAAGAGC

2.2.1 Making the SgRNA compatible with the target site

The sgRNA in its raw form would not be useful unless cloned in to a plasmid (Annex III) and later transcribed to RNA. To do that, the SgRNA needed to be compatible with the enzyme restriction zone. BsaI cut in 5' GGTCTC(N)$_1$ 3´ and in 3' CCAGAG(N)$_5$ 5'. Therefore, the SgRNAs need to have the necessary homology zones for later plasmid integration. To achieve homology between SgRNA and the target site an "TAGG" was added in the 5' to 3´region of the forward strand and "ACCC" to the 5' to 3´ region of the reverse stand. With the homology zone added to each respective side, the SgRNAs were ordered.

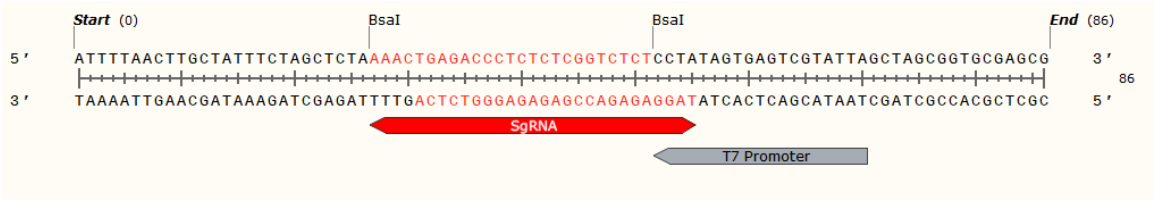

Figure 2.3. Region of pDR274 plasmid where BsaI restriction enzyme performances and where the SgRNA is inserted. The sequences in red represent the local where the SgRNA inserts and also shows the necessary homology arms.

2.3 Designing primers to amplify the SgRNAs target zone

The primers were created using the NCBI primer blast (https://www.ncbi.nlm.nih.gov/tools/primer-blast/). I inserted the sequence of interest, and selected the range which the primers should amplify. There range of the PCR product size was between 70 bp to 200 bp and the melting temperature between 63ºC (minimal) 65ºC (optimal) and 67ºC (maximum) The genome data base was changed from "Refseq mRNA" to "Genome (reference assembly from selected organisms)" and the species to "*Danio rerio*

(Hamilton, 1822) (taxid: 7955)". On the advance parameters, the primers size was designated to 21 (minimal), 23 (optimal) and 25 (maximum).

After being redirected to the new page, the pair of primes that suited better the situation was chosen. Meaning that the position and melting temperatures of the primers were taken into account. The temperature of each primer pair should be as close to each other as possible. The self-complementarity was also taken in to account.

Table 2.3. Primers used to amplify the regions of interest of *dnah7* and *rsph4a*

Target gene	Forward strand (5´ to 3')	Reverse strand (5´ to 3')	PCR product size
Dnah7 Sg1 (version 1)	TGTACTCAGAATGGCCTGGCCC	CGTCTGACCTTCTCCTGCTGGG	94
Dnah7 Sg1 (version 2)	TGCAGTCTTTACTGTGATCCCTGCC	AAAGGCTCAGCACTTTCTGCACG	171
Dnah7 Sg2	CCACCCTTGAACGTGTTTGTGAGGAGT	CAACTTCCCTGTGGCTGTGCTG	105
Rsph4a Sg2	TTTCTTTGAGCAAGCTGGCGTGG	CCTTCCGCCACCAGGTAGTTTCC	153

2.4 SgRNAs annealing and integration on pDR274 plasmid

To perform the junction of both strands of DNA, SgRNA forward strand and SgRNA reverse strand, 5 µl of each strand was added in an eppendorf with 24 µl of annealing buffer and 23 µl of Milli-Q water. The reaction tube was then placed on a thermoblock at 95°C for 5 min and let to cool down at room temperature. To avoid evaporation all tubes were wrapped with parafilm. The annealing buffer consisted in 10mM of Tris, 50 mM of NaCl and 2mM of EDTA. Afterwards, the SgRNAs were diluted 1:10 in Milli-Q water.

The pDR274 linearization was made using BsaI enzyme, which cuts in two places in the pDR274 plasmid guaranteeing that the SgRNA integration would be only in one direction and that the plasmid itself would not close. The linearization of the plasmid was made overnight at 37°C and confirmed using a 1% agarose gel. The plasmid was cleaned and concentrated using a DNA clean & concentrator™ kit by ZYMO RESEARCH™. With Nanodrop spectrophotometer for nucleic acid and protein quantitation the exact concentration of the plasmid was known.

With the SgRNAs and pDR274 prepared both were joined in a ligation reaction. In an Eppendorf, 0,33 µl of pDR274 plasmid (at 100ng/µl), 1,5 µl of the diluted SgRNA (1:10), 5 µl of 2x T4 buffer, 1 µl of T4 ligation enzyme were added and the tube filled with Milli-Q water until a volume of 10 µl is reached. Incubated overnight at 16°C.

2.5 Bacterial transformation

The bacterial transformation was performed using DH5α competent cells (*E. coli* strain). The cells were stored in 1, 5 ml eppendorf at -80°C. The DH5α cells were defrosted on ice for 20 minutes and the pDR274 plasmid with the SgRNA was added to the eppendorf and stayed on ice for more 30 minutes. The cells were heat-shock treated, 1 minute at 42°C followed by to 2 minutes on ice. After the heat-shock treatment, 1 mL of LB (Luria broth) medium, previously heated, was added followed by an incubation at 37ºC for 1 hour and 30 minutes at 250 RPM. Next, the cells were centrifuged at 5000 RPM for 10 min. The medium was discarded and the pellet was carefully resuspended in the remaining medium in the 1.5 ml eppendorf. The bacteria were plated in LB agar plates with Kanamycin (50ng/ µL) and left to incubate overnight at 37ºC, for no more than 16 hours.

2.6 Colony PCR

The objective of the colony PCR was to identify which of the individual colonies had the plasmid with the SgRNA incorporated. Using the plates with the transformed bacteria, each plate corresponded to is respective SgRNA, SgRNA 1, 2 and 3 for *dnah7* and SgRNA 1 and 2 for *rsph4a*. An individual colony was picked, with a micropipette tip, and dropped in a PCR tube filled with PCR mix. This process was repeated several times for each SgRNA, assuring that each SgRNA had at least 5 individual colonies. Next, I removed the tip from the PCR tube and plated the product in one quadrant of a previously divided LB agar plate. The primers were added: m13R was used as the forward primer and as a reverse primer, the forward strand of each SgRNA oligo was used. As for the controls, two positive controls were used one with M13R and pDR274_c3pcr3F and the other with M13R and pDR274_c3pcr3R. As for the negative control, it was used a blank tube without DNA, but with PCR mix and M13R and pDR274_c3pcr3F primers.

2.6.1 Bacterial liquid suspension

In the event of positive colonies, analyzed by electrophoresis in a 1% agarose gel at 100 Volts, those colonies were then replicated in a 15ml falcon with of LB medium with kanamycin at 50ng/ µL. The colonies were then incubated at 37ºC overnight, no more than 16 hours.

2.6.2 Preparation for sequencing

A Mini-prep kit ™ kit by ZYMO RESEARCH™ was used to prepare the DNA samples. Afterwards a nanodrop spectrophotometer quantification was made. All samples were diluted to reach Stabvida, Lda concentration guidelines of 100 ng/µl and were sent for sequencing.

2.7 In vitro DNA transcription

After sequencing and guaranteeing that the SgRNA integration in the pDR274 plasmid was successful, the DNA was transcribed into RNA. First, a mix of 15 µl of H_2O ,10 µl of transcription buffer 5X, 5µl DTT and 5µl NTP was prepared and incubated at 37ºC for 5 minutes. Afterwards 12 µl of DNA was added to the mix and incubated for 1 minute, at 37ºC. Next, 1 µl of RNA inhibitor was added and again incubated for 1 minute at the same temperature. The next step consisted in adding 1 µl of RNA polymerase and proceed with the incubation for one hour. In the next hour, 2 µl of RNA polymerase where added again in the mix and the incubation proceed for one more hour. At last, 1µl of Dnase was added to the mix and incubated for 30 minutes. To check if the reaction was successful the samples were run in a 1% agarose gel.

2.8 Preparing the SgRNA for injecting

The RNA was cleaned using a RNA clean & concentrator™ kit by ZYMO RESEARCH™ and the RNA concentration was measured in a nanodrop spectrophotometer. With the concentrations known, I then mixed 100ng/µl of Cas9 mRNA with 50ng/µl of SgRNA.

2.9 Zebrafish maintenance

General maintenance, breeding and egg bleaching were carry out by two technicians at CEDOC´s fish facility. All procedures were made and according to the DGAV.

2.9.1 Zebrafish breeding

To breed zebrafish, wild type males and wild type females are removed, with a net, from the main facility tanks, and put together in a breeding box, normally in the evening. The breeding box consists in a small acrylic container, a sieve to prevent the adult fish from eating their own progeny, a transparent divisor

to allow visual contact, but no physical contract and a lid to avoid the fish jumping off the breeding box. With the breeding box assembled and filled with water, an individual male is placed on one side of the divisor and one or multiple females are placed on the opposing side, up to two can be put simultaneously. The breeding box is closed and left overnight in the dark. On the following morning, the divider is removed and used to create slight slope, which helps to simulate the slope in a river bank, facilitating the breading process. If the zebrafish male and female engage in courtship behavior, the female will start spawning eggs and the male will externally fecundate the eggs, by releasing the sperm in to the water. The eggs will sink through the sieve and deposit in the bottom of the box. The fishes are removed from the breeding box and put back in the same main facility tank and a label is placed in the tank indicating the day of the crossing. The eggs are collected by pouring the water from the breeding box with the eggs into a strainer, and then removing the eggs attached to the strainer by squirting embryonic medium (5 mM NaCl, 0.2 mM KCl, 0.3 mM $CaCl_2$, 0.3 mM $MgSO_4$, ddH_2O – pH 6.5). The eggs are collected in a petri dish filled with embryonic medium. To maximize the survival rate, each petri dish is filled with 50 to 100 eggs. With the eggs collected, each petri dish is identified with a name of the fish lines crossed, date, researchers name and other relevant information. At this point the eggs can be used right away for experimental procedures or left in an incubator at 25ºC or 28ºC until the desired developmental stage is reached.

2.9.2 Relocating the fish from petri dishes to the main facility tanks

To move the embryos from the petri dishes to the main facility tanks, they need to be bleached, while they are still inside the chorion so that any harmful bacteria do not get introduced in the main system. This procedure is made by the fish facility technicians.

2.10 SgRNAs and MOs microinjections

The microinjections of SgRNAs and MO were made with a Nikon microinjector coupled with an PV820 Pneumatic PicoPump pressure injector (World Precision Instruments, Inc.;(Sarasota FL) and 50x Nikon SMZ745 zoom stereomicroscope. The microinjector is a Three-axis micromanipulator (Nashige, Greenvale, NY) and is used to manipulate a fine needle which is filled with SgRNA or MO solutions. The needle calibration can be done before or after the fish start laying eggs. Usually, it is recommended that the calibration is made before crossing the fishes or between the time that the divisor is removed and the fish start laying eggs. This way we can ensure that the eggs are injected in one cell stage, therefore the delivery and uptake of the SgRNAs or MO is made by only one cell, minimizing mosaicism. If the calibration is made after the laying, it needs to be done quickly, so that injecting the embryos starts within the 40 minutes time window between one cell stage and two cell stage.

The calibration is made by putting a drop of oil above a S1 stage micrometer ruler (10mm/0.1mm Graticule Ltd., Tonbridge, Kent) and pumping 10 times into the oil, the goal is to create a 0.3 nm diameter

bubble with 10 pumps. This allows to calculate the volume of each individual pump. Knowing that with 10 pumps the bubble occupies 0.3 nm, in diameter, we can calculate the sphere volume. This way we know that each pump injects 1.4 nL of solution in to the egg. To reach 0.3 nm bubble with 10 pump, the needle tip is broken by small increments using tweezers or by adjusting the duration and/or the eject pressure of each pump in the Pneumatic PicoPump pressure injector.

When calibrated, the embryos are slowly positioned against a microscope slide in a petri dish lid and all excess embryonic medium is removed to prevent embryo rotation or any undesirable movements of the embryo when in contact with the needle. The needle is positioned in an angle and pointed to the center of the embryo. For each injected embryo, the needle is moved back while the petri dish moved up and the position of the needle is then restarted. Each injection is made in the yolk. Afterwards the injected embryos are relocated to a new petri dish with embryonic medium and placed in an incubator at 25ºC.

2.11 DNA extraction of SgRNA injected embryos

The potential mutants were screened, 24 hours post injection, with 8 embryos randomly selected, per petri dish, and their DNA was extracted. These 8 larvae are gathered in a 1.5 ml Eppendorf and the excess embryotic medium is removed and 20µl of NaOh (50Mm) is added. The Eppendorf is incubated at 96ºC for 20 minutes followed by another incubation at -4ºC for 20 minutes. Between the incubations, the embryos were smashed to provoke cell lysis. After both incubations, 2µl of Tris-HCl (1M, pH8) was added followed by a 10 minutes centrifugation at 13200 RPM. To conclude the DNA extraction, the supernatant was removed, with special attention to not touch the pellet with all the cell debris, and placed in a new 1,5 ml Eppendorf and stored at -20ºC.

2.12 PCR

The DNA extracted from the 8 injected embryos was used in a standard PCR. The following table shows the components and quantities of the master mix used and the PCR temperature protocol.

Table 2.4. Master mix used for *dnah7* and *rsph4a* colony PCR.

Mix components	PCR mix (1x)
Buffer	2,5 µl
Dntps	0.5 µl
$MgCl_2$	1,25 µl
Primer F 1	0.5 µl
Primer R 2	0.5 µl
Taq polymerase	0.2 µl
Sample (gDNA)	- µl
H_20	19.55 µl
Total	25 µl

Table 2.5. PCR temperature protocol used for *dnah7* and *rsph4a* colony PCR.

	Temperature	Time	Cycles
Initial denaturation	95°C	10 min	---
Denaturation	95°C	60 sec	30
Annealing	61-51°C	60 sec	30
Elongation	72°C	60 sec	30
Final extension	72°C	10 min	---
Storage	12°C	infinite	---

Table 2.6. Master mix used for *dnah7* SgRNA1 and 2 PCRs.

Mix components	PCR mix (1x)
10X Buffer	2,5 µl
Dntps	1.25 µl
$MgCl_2$	1,25 µl
Primer F 1	0.5 µl
Primer R 2	0.5 µl
Nzt taq polymerase	0.2 µl
Sample (gDNA)	1 µl
H_20	17.8 µl
Total	25 µl

Table 2.7. PCR temperature protocol used for *dnah7* SgRNA1[(1)] and SgRNA2 [(2)].

	Temperature	Time	Cycles
Initial denaturation	95°C	10 min	---
Denaturation	95°C	20 sec	39
Annealing	56[(2)]/61°C [(1)]	30 sec	39
Elongation	72°C	45 sec	39
Final extension	72°C	10 min	---
Storage	12°C	infinite	---

Table 2.8. Master mix used for *dnah7* SgRNA1 new primers.

Mix components	PCR mix (1x)
Buffer	5 µl
Dntps	0 µl
$MgCl_2$	0 µl
Primer F 1	1 µl
Primer R 2	1 µl
Taq polymerase	0.25 µl
Sample (gDNA)	1 µl
H_20	16.75 µl
Total	25 µl

Table 2.9. PCR temperature protocol used for *dnah7* SgRNA1 new primers.

	Temperature	Time	Cycles
Initial denaturation	95°C	1 min	---
Denaturation	95°C	15 sec	35
Annealing	70°C	15 sec	35
Elongation	72°C	10 sec	35
Final extension	72°C	3 min	---
Storage	16°C	infinite	---

Unfortunately, the first set of primers used for amplifying *dnah7* SgRNA1 stopped amplifying. They were promptly replaced with new primers, with a bigger PCR product but, still amplified the same region.

2.13 Polyacrylamide gel electrophoresis (PAGE) for mutant detection

A polyacrylamide gel electrophoresis was utilized to detect the presence or absence of mutant DNA caused by the SgRNAs microinjections. The PAGE consists in a polyacrylamide mesh, which when applied a voltage, can separate fragments by their size. When applied a voltage, the negative charged fragments, in this case DNA fragments, migrate in the direction of the opposing charge. Therefore, bigger fragments have more difficulty migrating through the gel, while smaller fragments migrate easier, thus migrating further in the gel.

The goal of the SgRNAs is to cause a double strand break in the zebrafish genomic DNA and, hopefully, lead to a non-homologous end joining recombination which can lead to insertions or deletions on the genomic DNA. These insertions and deletion are detected trough PAGE, since they generate heteroduplexes causing the mutated DNA to migrate at a different rate than the wild type DNA. Heteroduplexes occur when the forward strand and the reverse strand are not 100% complementary but, still present sufficient complementarity to form a duplex. By having a mismatch in one or more base pairs, these heteroduplexes migrate slower through the gel than the homoduplexes from the wild type DNA, that have 100% complementarity.

To set up a PAGE all the necessary components were gathered. The short and top glass plates were cleaned with 70% ethanol, aligned and put in a casting frame. The casting frame was then put in a casting stand. The 15% polyacrylamide gel was prepared by adding 6.170 ml of Mili-Q water, 1.2 ml TBE buffer 10x, 4.5 ml of acrylamide/bis-Acrylamide (29:1 solution; Nzytech MB04501), 120 µl of ammonium persulfate and 9,6 µl TEMED in a 15 ml falcon. Between adding each reagent, the falcon was slowly inverted a couple of times to mix the reagent properly. The TEMED reagent was added inside a HOTT since, it is a very toxic reagent. Immediately after adding and mixing the last reagent, the mixture was put in between the glass plates, with and electric accurpette, and a comb placed. In the 15 to 20 minutes that takes the polyacrylamide gel to polymerize, the samples were prepared. After

polymerizing, the comb was carefully removed, the casting frame was detached from the casting stand and the glass plates removed from the framing stand. The glass plates were placed in a support that went inside the electrophoresis chamber. The chamber was filled with TBE running buffer (1X) and an ice pack was place inside to prevent overheating. Before loading the gel, the wells were cleaned by doing an up and down with a pipette. The polyacrylamide gel was loaded with 6 µl of PCR product with 0.6 µl of loading buffer (6X) and one well with 2 µl of gene ruler ladder. The chamber was connected to the power supply. The power supply was set up to 150 Volts for 3 hours. After 3 hours, the power supply was turned off and the gel removed from the glass plates with extra caution to avoid ripping or damaging the gel. The gel was placed in a resolving solution, consisted by 2 µl of GreenSafe Premium (Nzytech MB13021) and 50 ml of TBE running buffer (1X), were it reveals for 10 minutes. Two optional washes with ddH_2O, 5 minutes each, can be made to eliminate any excess GreenSafe in the gel, resulting in a shaper picture. The picture was taken using a Molecular imager ® ChemiDoc ™ XRS Imaging system from Bio-Rad and ChemiDoc software.

2.13.1 Finding heteroduplexes

Whenever heteroduplexes were found, the corresponding batch of injected eggs was transferred to the main facility tank, after no longer than 6 days of staying in a petri dish.

2.14 Microscopy setup to image moving cilia in live embryos

The microscopy setup consisted in a Nikon Eclipse Ti-U inverted brightfield microscope coupled with high speed FASTCAM MC2 camera (Photron Europe, Limited). A Pan Fluo 100x /1.30NA oil immersion objective was used. The software used was PFV (Photron FASTCAM viewer).

2.14.1 Mounting live zebrafish embryos for cilia beat frequency recording

To obtain the CBF at 48 hpf the larva were treated with an melanogenesis inhibitor, 1-phenyl 2-thiourea (PTU sigma), otherwise would be impossible to visualize the ciliary beating due to the development of the skin pigmentation. The PTU was added at 24 hpf. To mount the larvae a mold was used which consisted of 2% agarose mixed with embryotic medium. The mold had wells where the larva were placed and handled with extreme caution, since at this stage they are very fragile and can be killed or damaged with ease. To immobilize the larvae, tricaine 1X was used. The larvae where positioned in a way that the tail was against the glass bottom of the Fluorodish™ for World Precision Instruments Inc, China. With this setup, the larvae where kept alive and immotile during the video capture and the tail stayed always in focus.

2.14.2 Video acquisition - Recording cilia present in the tail end

Before starting recording cilia, it was important the know the number of frames per seconds necessary to capture the CBF optimally. The unit frame per second (FPS) refers to the images that the camera captures per one second. Capturing images with higher FPS allows visualization of quick events in slow motion therefore, we can analyze these events in greater detail. The CBF measurements were dependent on the frame rate used. A too low FPS will not provide the necessary detail for CBF measure and a too high FPS will reduce the resolution and brightness of each picture, because to capture more images in a second the resolution needs to be lower due to camera limitations and the brightness is lower as well, since there is less time for the light to be in contact with the sensor, resulting in loss of image quality. Therefore, the right balance needs to be achieved between FPS used and the speed of the event. To achieved that balance, we followed the *Nyquist-Shannon* sampling theorem which says that to capture the frequency F_0 of cilia, the image should be acquired at a rate twice as fast as the native cilia frequency (Jaffe et al., 2010). This condition is necessary to remove any aliasing (motion artifacts). So, we opted to capture at 250 FPS during 1000 frames, which at 250 FPS is 4 seconds. At this rate, we would be recording with 70 more frames that the recommend 180 FPS.

2.14.3 Video processing

All the video processing was made using ImageJ software (https://imagej.nih.gov/ij/). To analyze the Cilia Beat Frequency (CBF) all videos were stabilized using the registration plugin present in ImageJ. This eliminated any unnecessary motion, like the hearth beat, allowing a smoother and more accurate analysis of the CBF. Next, we used the CiliarMove, a software created in the Lopes lab tailored to analyze CBF in a standard and faster way.

2.15 Statistical analyses

All statistical analyses referent to CBF comparison were made using the software *GraphPah – Prism*® version 5.0 (GraphPad Prism Software Inc. San Diego, CA). *GraphPah* used to compare data sample using parametric tests (T test). All values were considered significantly different when *p* value is below 0.05.

3. Results

From the four goals conceived in the beginning of this thesis, three are still ongoing and one was only partiality achieved. All the goals related to the creation of mutant lines were severely affected by the lack of reagents in the lab due to a change in NOVA University fiscal status that became a Foundation. This meant that when important reagents, like TAQ polymerase for PCRs, TBE buffer for running agarose gels and PAGE gels finished the screening was stopped. Other reagents like T7 RNA polymerase necessary for RNA transcription, were severely delayed after being ordered months before, delaying the injection of SgRNAs. Furthermore, the fish facility suffered from a heat stroke in the previous year which provoked bad postures throughout the rest of 2016, delaying even more the injections of the SgRNAs. Therefore, all CRISPR-Cas9 goals are still ongoing meaning that remaining crispants still need to be screened in the future and *rsph4a* SgRNAs need to be transcribed and injected in the near future.

3.1 Confirming the linearization of pDR274 with BsaI restriction enzyme

To produce to CRISPR-Cas9 mutants, I linearized the plasmid so that the SgRNA could then be inserted and reclose the plasmid upon junction. The utilization of BsaI restriction enzyme allows the SgRNA to be inserted in only one direction, since BsaI cuts the plasmid in two distinct zones creating two distinct homology zones, which the SgRNA has a complementary homology arm that matches for each of the homology zones.

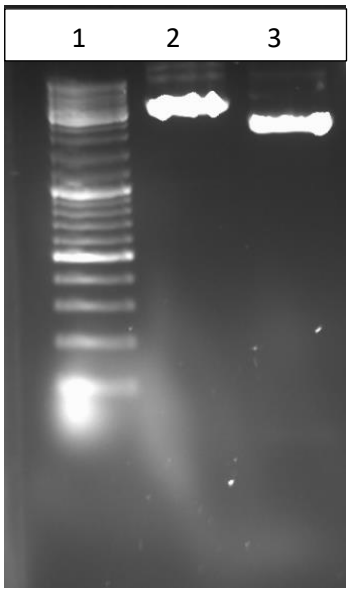

Figure 3.1. 1% agarose gel used to check pDR274 plasmid linearization with BsaI restriction enzyme. Gel sample order: (1) 100 bp ladder, (2) linearized pDR274 plasmid, (3) circular pDR274 plasmid.

The linearization was confirmed using electrophoresis. In the first lane of the 1% agarose gel, a 100 bp ladder was loaded, followed by the linearized pDR274 plasmid and then the circular plasmid. The expected results were that the linearized plasmid would migrate slower through the gel, therefore

traveling less distance than the circular plasmid. This is due to the plasmid conformation, since they are equal in size, the only factor to take into account is the plasmid conformation. A circular plasmid, in vivo, is a compact structure referred as supercoiled. A supercoiled plasmid creates less resistances when migration in a gel matrix, due to his compact structure. On the other hand, a linear plasmid is a long strand of DNA and presents greater resistance when traveling through the gel. The circular plasmid traveled further than the linear one, confirming that the plasmid linearization was successful.

3.2 Colony PCR results

After the junction of the linearized plasmid and each SgRNA. The plasmid with the SgRNA was ready to be cloned. For that a colony PCR was used. This technique allowed to clone the plasmid and by means of electrophoresis verify the success of the junction between plasmid and SgRNA. An agarose gel would indicate the presence of the SgRNA in the plasmid, if the band corresponded to the PCR product matched the predicted product. The predicted PCR product is the number of base pairs between the primers used to amplify the DNA. In the case of Colony PCR, the number of base pairs between M13 primer and the respective forward strand of each SgRNA that was used as a primer. If the SgRNA was inserted correctly, then the forward strand of each SgRNA would match the reverse strand in the plasmid and thus amplifying the PCR product.

3.2.1 Colony PCR for *dnah7*

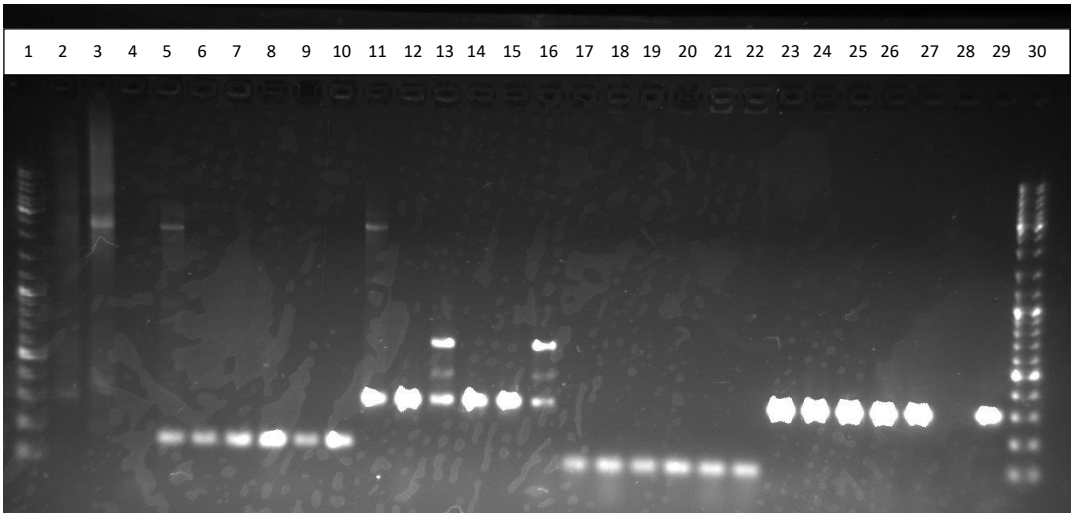

Figure 3.2. Agarose gel at 1% to check *dnah7* SgRNA colony PCR results. Gel sample order: (1) 100 bp ladder, (2) postive control 1, (3) positive control 2 , (4) negative control , (5 -16) 5th to 16th well are non related smaples, (17) SgRNA1 colony 1, (18) SgRNA1 colony 2, (19) SgRNA1 colony 3, (20) SgRNA1 colony 4, (21) SgRNA1 colony 5, (22) SgRNA1 colony 6 , (23) SgRNA2 colony 1, (24) SgRNA2 colony 2, (25) SgRNA2 colony 3, (26) SgRNA2 colony 4, (27) SgRNA2 colony 5, (28) empty well, (29) SgRNA2 colony 6, (30) 100 bp ladder.

This agarose gel (Figure 3.2) showed that all the samples referring to SgRNA1 were negative. The expected molecular weight (around 300 bp) did not match what was observed in the gel, which was

around 100 bp. On the other hand, all the samples for SgRNA2 matched the predicted molecular weight of 300 bp apart from colony 5 which did not amplify. As for the positive controls, none of them seemed to amplify in the correct region. Although, a faint band could be seen in the region of 300 bp, for the positive control 1, it did not match the expected molecular weight of 180 bp. The negative control showed no signs of contamination. Even with both positive controls, negative, we still processed to the next step. Since there was a band in the correct zone for all SgRNA2 samples, indicating SgRNA integration.

Due to time constrains the colony PCR for SgRNA1 was not repeated. Instead the Colony PCR was bypassed and new colonies were picked for a bacterial suspension and sent directly for sequencing after the DNA extraction and purification.

The third SgRNA for *dnah7* was eventually dropped, after three colony PCRs, where none of the colonies picked showed amplification.

3.2.2 Colony PCR for *rsph4a*

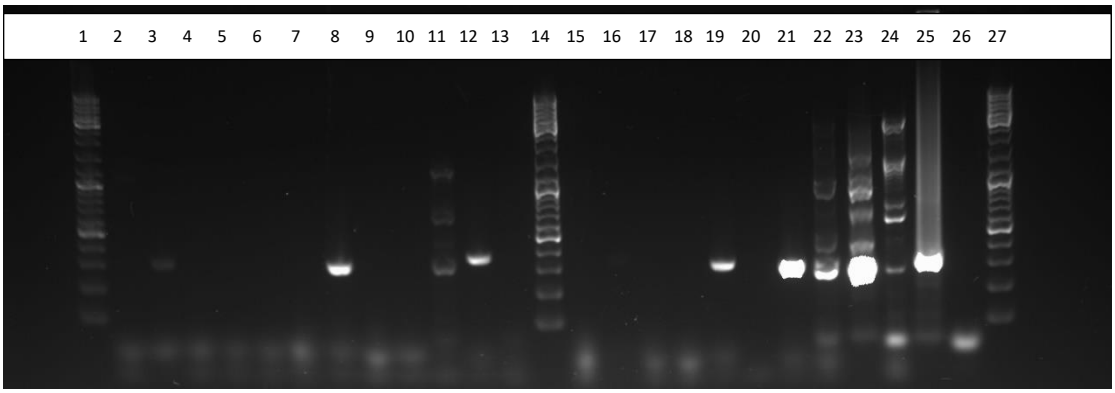

Figure 3.3. Agarose gel at 1% to check *rsph4a* SgRNA colony PCR results. Gel sample order: (1) 100 bp ladder, (2) SgRNA1 colony 1, (3) SgRNA1 colony 2, (4) SgRNA1 colony 3, (5) SgRNA1 colony 4, (6) SgRNA1 colony 5, (7) SgRNA1 colony 6, (8) SgRNA1 colony 7, (9) SgRNA1 colony 8, (10) SgRNA1 colony 9, (11) SgRNA1 positive control 1, (12) SgRNA1 positve control 2, (13) SgRNA 2 negative control, (14) 100 bp ladder, (15) SgRNA2 colony 1, (16) SgRNA2 colony 2, (17) SgRNA2 colony 3, (18) SgRNA2 colony 4, (19) SgRNA2 colony 5, (20) SgRNA2 colony 6, (21) SgRNA2 colony 7, (22) SgRNA2 colony 8, (23) SgRNA2 colony 9, (24) SgRNA2 positive control 1, (25) SgRNA2 positve control 2, (26) SgRNA2 negative control, (27) 100 bp ladder.

In the Figure 3.3, the first group of samples referring to *rsph4a* SgRNA1(2nd to 12th well) showed mostly negative results for all colonies except for colonies 2 and 7. Both colonies presented bands in the 300bp region which matched the predicted molecular weight. The positive controls for the group of samples had mixed results. Positive control 1 presented multiple bands, which extended from 300 bp to 1000 bp. Positive control number 2 was positive, showing a band in the correct region, around 340 bp. The second group of samples referred to *rsph4a* SgRNA2 (14th to 25th well) showed positive results for four colonies, colony 5 ,7, 8 and 9. They all had an intense band in the 300 bp region especially colonies 7 and 9. However, colony 8 and 9 had multiple bands. This time both positive controls showed troublesome results. Both controls had the expected band, but control 1 also had more bands in non-expected areas, and positive control 2 has a smear, which maybe a sign for DNA degradation. In both groups the

negative controls showed no sign of contamination. Either way, all the colonies, which had a band in the 300 bp region, were sent for sequence after DNA purification, and quantification.

3.3 Sequencing results

By sequencing the PCR product of the colony PCRs, after proper sample treatment, I knew if the SgRNA was inserted the plasmid. In theory, it should be, since, like it was previously mentioned, the amplification of colony PCR only happens if the forward strand of each SgRNA, used as a primer, finds its complement in the plasmid. Either way, all positive samples from the colony PCR were sequenced.

Figure 3.4. Alignment between pDR274, pDR274 with each respective SgRNA and each individual SgRNA. (A) Alignment between pDR274, pDR274 inserted with *dnah7* SgRNA1 and *dnah7* SgRNA1. (B) Alignment between pDR274, pDR274 inserted with *dnah7* SgRNA2 and *dnah7* SgRNA2. (C) Alignment between *rsph4a* SgRNA2, pDR274 and pDR274 inserted with *rsph4a* SgRNA2.

After finding positive colonies for *dnah7* SgRNA2 and *rsph4a* SgRNA2, the respective samples were sent to sequence. As previously mentioned, *dnah7* SgRNA1 integration was not confirmed with colony PCR instead, the new colonies picked were directly sent to sequence. Figure 3.4, shows the alignment between the native pDR274 plasmid, pDR274 plasmid with a SgRNA inserted and the respective SgRNA. “A”, “B” and “C”, shows a 100% match between the native SgRNA and the SgRNA interest in to the plasmid.

3.4 Confirming the linearization of pDR274 with Hind III restriction enzyme

Once confirmed the correct SgRNA sequence is in the plasmid, the plasmid was re-opened using Hind III restriction enzyme. In contrast with bsaI, this restriction enzyme only cuts in one zone. Like before

the linearization was checked using electrophoresis. A positive result meant that the plasmid would be ready to be transcribed to RNA. When transcribed into RNA the SgRNA would be ready to inject.

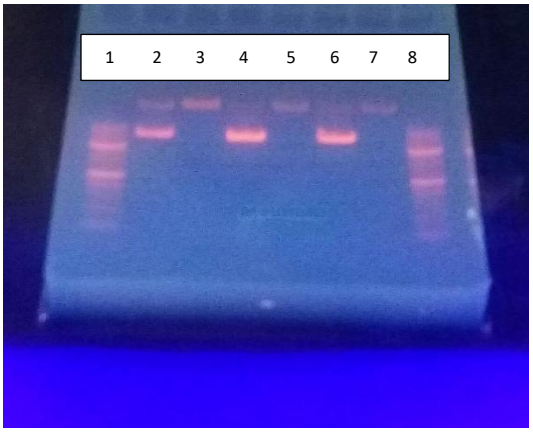

Figure 3.5. 1% agarose gel used to check pDR274 plasmid with *dnah7* SgRNA1 linearization with Hind III restriction enzyme. Gel sample order: (1) 100bp ladder, (2-5) 2nd to 5th well are non-related samples, (6) circular plasmid, (7) linear plasmid, (8) 100bp ladder.

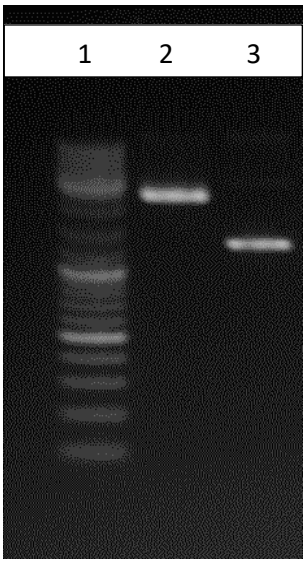

Figure 3.6. 1% agarose gel used to check pDR274 plasmid with *dnah7* SgRNA2 linearization with Hind III restriction enzyme. Gel sample order: (1) 100bp ladder, (2) linear plasmid, (3) circular plasmid.

Results presented in Figure 3.5 and Figure 3.6, demonstrated the Hind III linearization was successful for pDR274 plasmid with *dnah7* SgRNA1 and SgRNA2, respectively. Once again, the linearization was successful, since the circular plasmid migrated further than the linearized one. Linearization with Hind III was necessary for in vitro transcription from DNA to RNA. There was no linearization of *rsph4a* SgRNA2. The development of SgRNA2 for *rsph4a* stopped after the sequencing results, due to time constrains and long waiting timings for new reagents to arrive. With *dnah7* SgRNA1 and SgRNA2 prepared and ready to use, the fish were injected.

3.5 PAGE screening for potential heteroduplexes

The preliminary screening for mutants was again done using PAGE. The goal was to find heteroduplexes, which would indicate the presence of indels in the genome of the extracted DNA from the injected embryos. If found, the fish from the correspondent batch would be let to mature for 3-4 months, depending on space availability and food intake, for later screening.

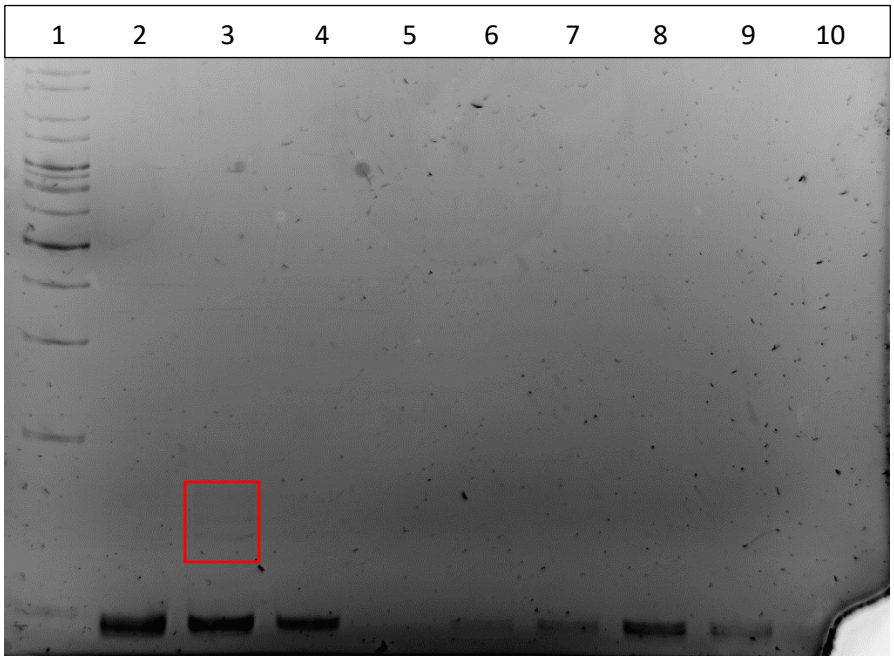

Figure 3.7. 15% polyacrylamide gel for early *dnah7* SgRNA1 mutant screening. Gel sample order: (1) 100 bp ladder, (2) non-injected embryos (control 1), (3) batch 1.1 of injected embryos, (4) batch 1.2 of injected embryos, (5) non-injected embryos (control 2), (6) batch 2.1 of injected embryos, (7) batch 2.2 of injected embryos, (8) batch 2.3 of injected embryos, (9) positive control for the PCR, (10) negative control.

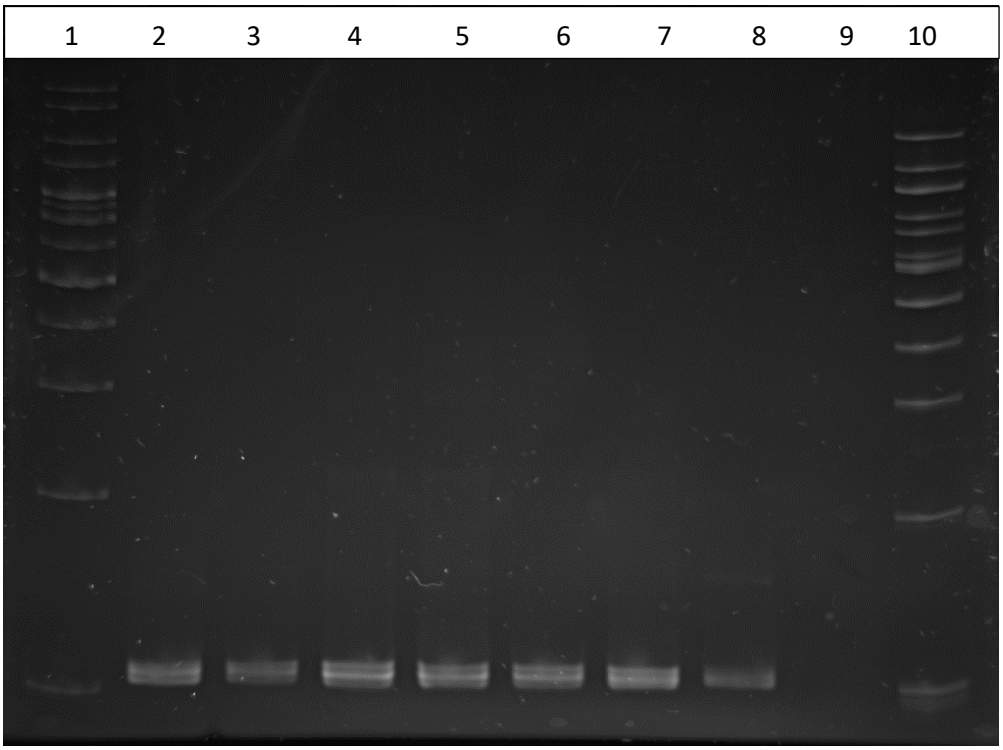

Figure 3.8. 15% polyacrylamide gel for early *dnah7* SgRNA2 mutant screening. Gel sample order: (1) 100 bp ladder, (2) non-injected embryos (control 1), (3) batch 1 of injected embryos, (4) batch 2 of injected embryos, (5) batch 3 of injected embryos, (6) non-injected embryos (control 2), (7) batch 4 of injected embryos, (8) PCR control, (9) negative control, (10) 100 bp ladder.

Results from Figure 3.7, were comprised by two different batches of embryos, batch 1 and batch 2, both with *dnah7* SgRNA1 injected fish. The control for batch 1, was positive, appearing a band below 100 bp which is concurrent with the expected 94 bp PCR product. This indicated a successful PCR and a correct amplification of PCR product for the wild type DNA. Furthermore, the control band helps to distinguish between wild type band and potential heteroduplexes. From the two batches referent to control 1, only in batch 1.1 could heteroduplexes be detected. The heteroduplexes can be seen above the band referring to the wild type (94 bp band) around the 150 bp ladder mark (red box). Although, the bands are faint, this can be explained by the low success rate in mutant creation. Meaning that, from the eight larva that each batch had, perhaps one larvae had the mutation, resulting in a faint band for the mutated DNA and a more intense band for the wild type DNA. With this finding, all the remaining embryos that were injected at the same time of batch 1.1, were bleached and reallocated into the main fish facility for later screening.

Batch 2 control, did not amplify, but the control from batch 1 could still be used to compare the wild type band. None of batch 2 samples demonstrated any heteroduplexes, only the wild type band. So, all the remaining fish larva were euthanized. The positive control for he PCR was used to check if the PCR itself worked, since this sample of wild type DNA worked previously. This was made to ensure that in case of failure in amplifying batch 1 and batch 2 DNA, the error was in the DNA extraction and not the PCR. The negative control didn't show any sign of contamination.

The screening for *dnah7* SgRNA2, came out negative for all samples. The positive control for wild type DNA had a band slightly above the 100 bp which was concurrent with the expected 105 bp. The PCR control and the negative control were both successful, showing a successful PCR and without contamination.

These results demonstrated that we were able to produce heteroduplexes in one batch of injected fish. Although, not all the PAGE gels are showed here, the only heteroduplex detected was from the batch 1.1 in Figure 3.7. All the other PAGE gels did not present any heteroduplexes.

3.6 Rearing Crispant fish until sexual maturation

After finding heteroduplexes for *dnah7* SgRNA1, fish from that batch were transferred in to aquariums where they would be kept until they reach full adulthood. Optimistically, this period would last three months. To speed up growing they were split into two tanks (Figure 3.9, A and B), resulting in a less crowed aquarium, and fed three times a day instead of two. These practices were made to try to speed up the sexual maturation process, since the next step of screening for mutation was depended in the ability of the fish to reproduce. The next screening would be made to the progeny of the cross between the crispants, the injected fish with possible mutations, and wild type fish. By screening the progeny, I would know if the mutation was present in the gametes, and whether it was passed along to futures generations.

Figure 3.9. Aquarium where the potential mutants were kept while in their sexual maturation phase. (A) Tank number 1 for zebrafish injected with *dnah7* SgRNA1 and screened by PAGE gel. (B) Tank number 2 for zebrafish injected with *dnah7* SgRNA1 and screened by PAGE gel. (C) Tank number 3 for zebrafish injected with *dnah7* SgRNA1 and screened by looking at L-R defects.

Tank C in Figure 3.9, is another batch of injected fish with *dnah7* SgRNA1. Although, these fishes were not screened by using a PAGE gel. Instead, they were screened by looking for laterality defects, curly up tails or heart edemas. This approach was designated, because heteroduplexes could not be identified due to lack of reagents in the lab.

This period of fish sexual maturation, was longer than expected, reducing the already short time frame for progeny screening. Furthermore, other complications arose in the same time frame worsening ever more the task at hand.

3.6 Screening *dnah7* "Crispants" by PAGE

Screening batch 1.1 progeny followed the same process as screening the injected embryos for mutations. Although the primers used for screening were different, since some complications arose with the old primers. Nonetheless, this new pair of primers was designed to target the same region as the older ones. The change in primers, did not influence the screening. This time, the expected PCR product would have 171 bp instead of 94 bp. The doubling in PCR product was to enable an easier detection of heteroduplexes since the previous primers would often be confused with primer dimers.

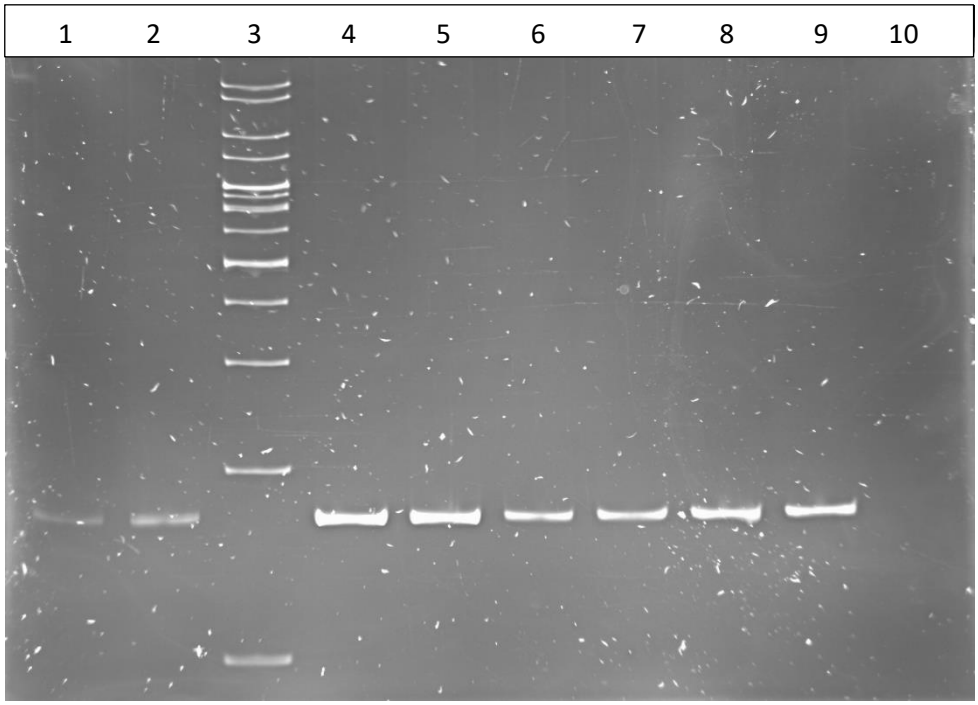

Figure 3.10. First 15% polyacrylamide gel for *dnah7* SgRNA1 "crispants" screening. Gel sample order: (1) wild type zebrafish (control), (2) Male 1, (3) 100 bp ladder, (4) Male 2, (5) Male 3, (6) Male 4, (7) Male 5, (8) Male 6, (9) PCR control, (10) negative control.

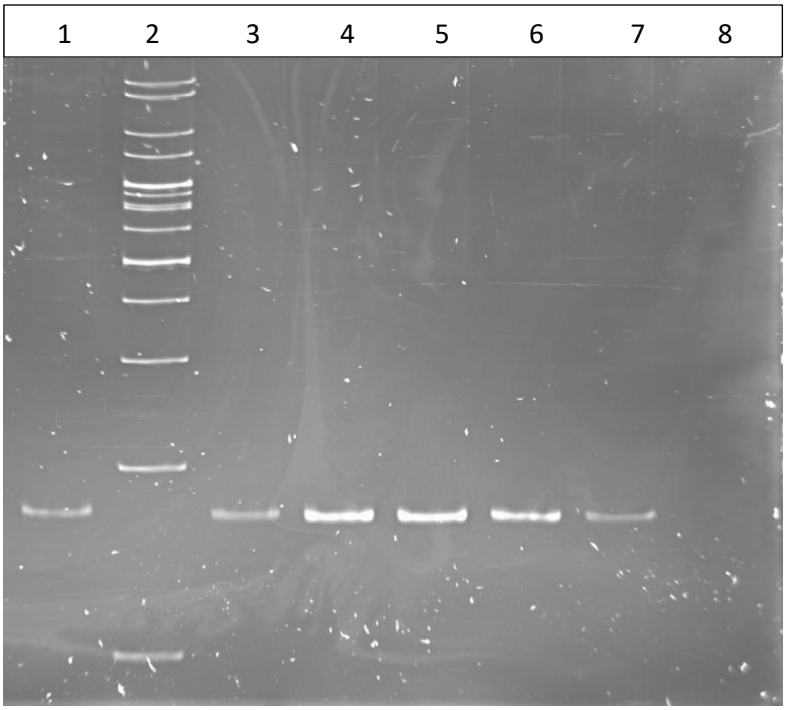

Figure 3.11. Second 15% polyacrylamide gel for *dnah7* SgRNA1 "crispants" screening. Gel sample order: (1) wild type Zebrafish (control), (2) 100 pb ladder, (3) Female 1, (4) Female 2, (5) Female 3, (6) Female 4, (7) Female 5, (8) negative control.

Both Figure 3.10 and Figure 3.11 represent the later stage of zebrafish screening. The samples are the DNA extracted from larva after the cross between the batch 1.1 and wild type. Screening in this way, would allow to detect mutations in the progeny of the early detected mutants, which would mean that the mutation was present on the gametes and could be passed along through generations. In Figure 3.10, the wild type DNA which is used as control, matched the predicted 171 bp by having a band around the same region. As for the DNA from the progeny of the Crispant, none of them demonstrated the formation of heteroduplexes. The same was seen in Figure 3.11, the controls matched the 171 bp region, and none of the other samples presented heteroduplexes. In both Figures the negative control was blank, showing no sign of contamination.

Unfortunately, the first round of screening did not yield any positive results. Therefore, all the fish were euthanized. The remaining fish were not screened due to a prolonged maturing stage, which reduced the screening time. However, these fish are going to be screened in the future by other students in the lab.

Consequently, in order to learn how to perform the functional studies on cilia beat frequency, a CBF analysis was done in wild type fish and fish injected with different MOs.

3.7 Cilia beat frequency analysis

Since, the end of the project could not be reached because the potential mutants needed more time to grow, we decided to evaluate the CBF in another model in order to learn a new technique. Initially, the

plan was to use *dnah7* MO to cause CBF disruption. But, the morpholino yielded unusual high mortality rates, that could range from 50 to 80%, depending on the batch, using a concentation previously tested to only cause a mortality rate of 15%. So, the possibility of comparing the wild type CBF to *dnah7* MO was dropped, as well as the comparison with the *dnah7* CRISPR mutant progeny, since they were still growing to reach the sexual maturation. Either way, an alternative was found and the *dnah7* MO was substituted by *ccdc40* MO. Similar to *dnah7*, this morpholino also created defects in left-right symmetry when injected in the correct concentration. Indicating a possible reduction in CBF due to low mobility, static cilia or the non-assembly of the correct dyneins along the axoneme of the cilia.

The analysis of the cilia beat frequency was made in the ependymal cells located in the spinal canal at the tip of the tail of a 48 hpf larvae. The cilia in this region were only developed at 48 hpf, any time earlier they were not found. The measurements were made in two zones, one closer to the tip of the tail and one further apart from the tip. The zone further from the tip of the tail was defined as the proximal zone (black arrow, image A, Figure 3.12), since the reference point was the head and not the tail, while the zone closer to the tip was defied as distal (red arrow, Image A, Figure 3.12).

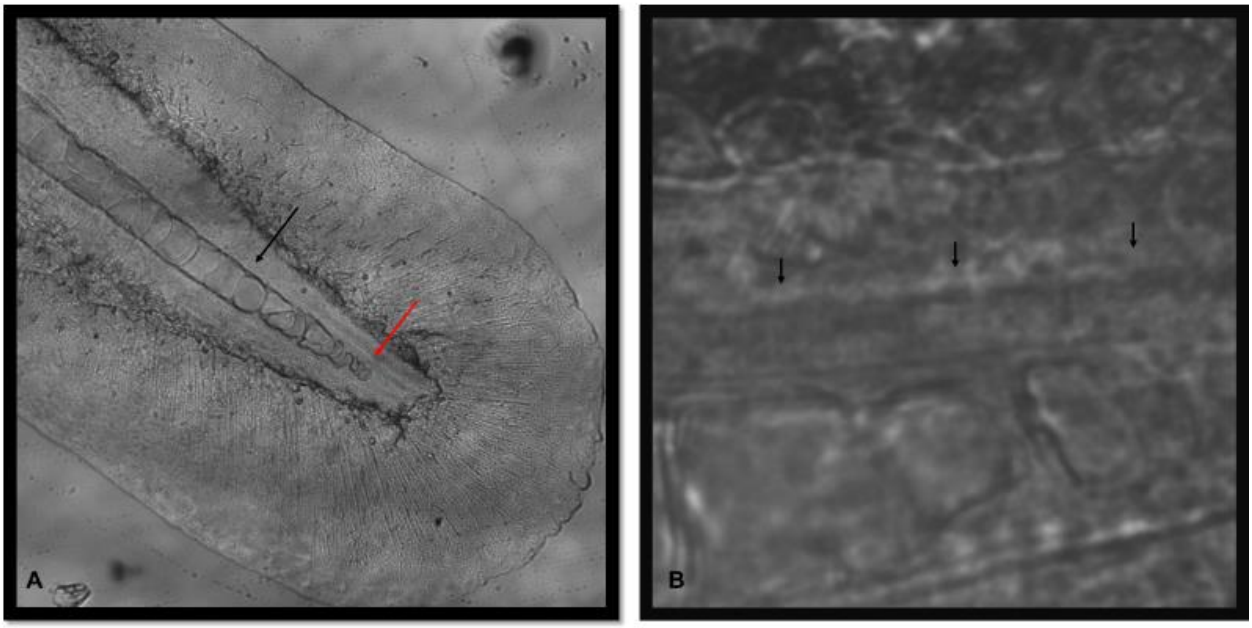

Figure 3.12. Microscope photographs of the end of the tail of a 48 hpf larvae. (A) Photo taken at 10X magnification of the end of the tail to demonstrate the proximal zone (red arrow) and the distal zone (black arrow). (B) Photo taken at 100x magnification of the proximal zone with the black arrows indicating the zone were all three measurements were taken.

Within each zone, three measurements were taken as can be seen in arrows from image B, Figure 3.12. A kymograph of the CBF, obtained thought plugins within ImageJ, was used to measure the CBF manually. Each peak in the kymograph was counted and the total was divided by kymograph duration resulting in a frequency. The digital measurements were made using the software CiliarMove. This

software would analyze the most recurrent frequency present in the video. The software would then originate a bar graph with all frequencies in “x” and in “y” its respective percentage (Figure 3.13).

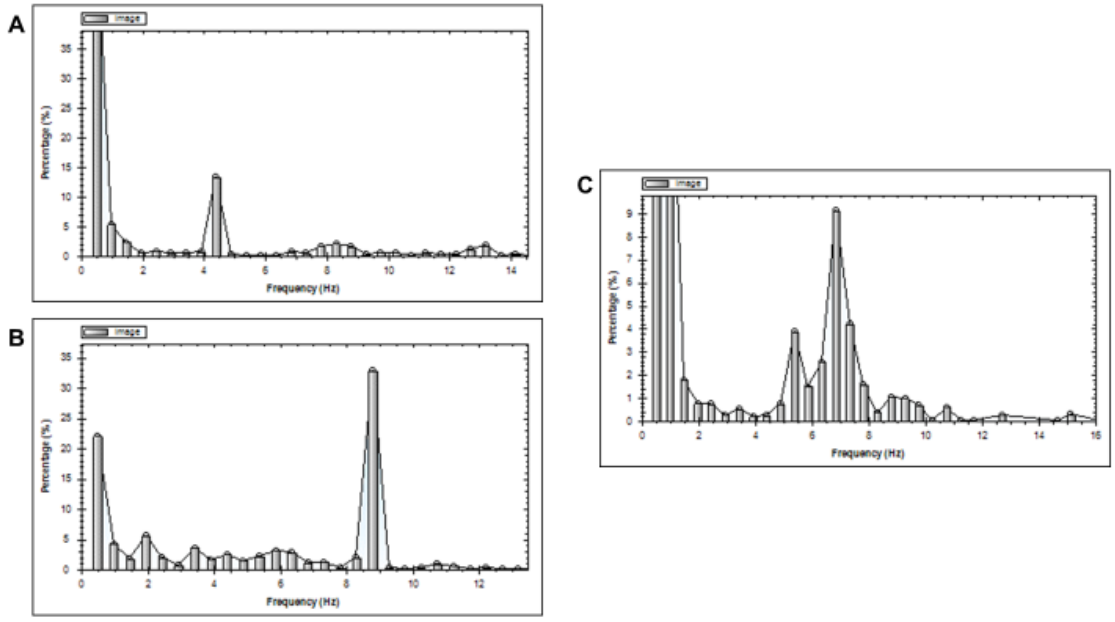

Figure 3.13. Graphical output from CiliarMove of one distal zone of one of the analyzed larvae. (A) Graphical output from the first measurement of the distal zone of larvae 6 with a most recurring frequency of 4,44 Hz. (B) Graphical output from the second measurement of the distal zone of larvae 6 with a most recurring frequency of 8.7 Hz. (C) Graphical output from the third measurement of the distal zone of larvae 6 with a most recurring frequency of 6,8 Hz.

The most recurrent frequency would be picked and the average of three measurements would originate the reported frequency of the proximal or distal zone. This process was made for ten wild type larva. Although, the final number of larva digitally analyzed was only seven, since the videos corresponding to 2 of the larva had excessive motion, distorting the ability to analyze CBF digitally. The videos for the third larvae could not be opened with software, resulting always in an error. The analysis of *ccdc40* MO injected larva was made in the same way, but only digitally. In contrast with wild type larvae, the *ccdc40* MO injected larva were not randomly selected. They were first screened for the presence of left-right defects or any other types of anomalies, such as heart edemas and curly up tails.

3.7.1 Wild type CBF analysis with manual measurements vs software measurements (CiliarMove)

As stated before a wild type CBF analysis was made manually and digitally. This arose from the necessity to establish the CiliarMove software as a trustworthy tool for CBF analysis in these cilia. A comparison was made to see if there were statistical differences between both types of methods used to measure CBF (Figure 3.14). CiliarMove was a software developed to be used as a diagnostic tool for

identifying potential patients that suffer from PCD. Since then, the software has been submitted to a peer reviewed journal and is waiting for the reviews.

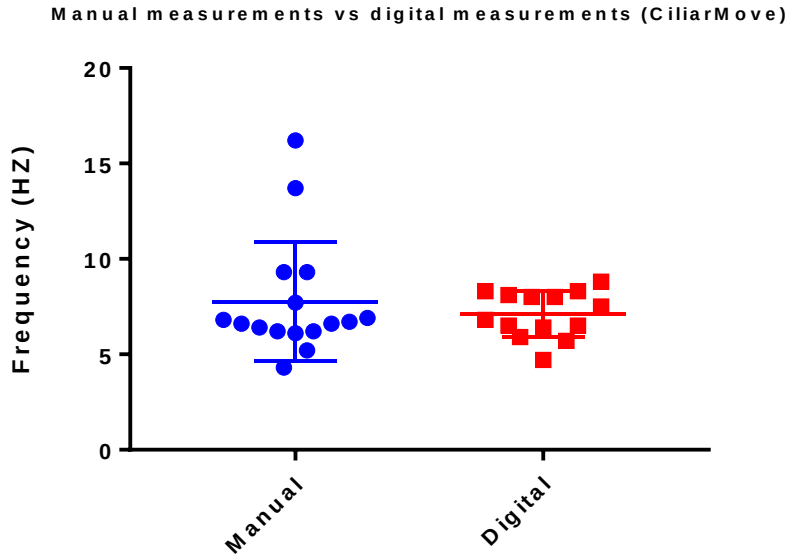

Figure 3.14. Graphical comparison between manual and digital CBF measurements of wild type fish. Scatter plot graphic comparing manual measurements (n=16) with digital measurement (n=14) of CBF in wild type fish.

A parametric test (student t test) showed that the difference between methods is not statistical significant. The *p* value of the t test was 0.4652 and data sets can only be considered significantly different when *p* value is below 0.05. The software measurements seem to be less error prone, by not having any outliers when compared do manual measurements. This would make sense, since there is the human element involved. We can conclude that there is not a difference in the data obtained using the distinct methods, therefore validating CiliarMove software for the zebrafish spinal canal cilia at 48 hpf.

3.7.2 Wild type CBF vs *ccdc40* morphants CBF

Since, Figure 3.14 showed that both methods yield data that is not statistical different, the analysis between wild type CBF and *ccdc40* MO injected larva was only made digitally. Figure 3.15 shows the result from the comparison of proximal and distal zones from wild type and *ccdc40* injected fish.

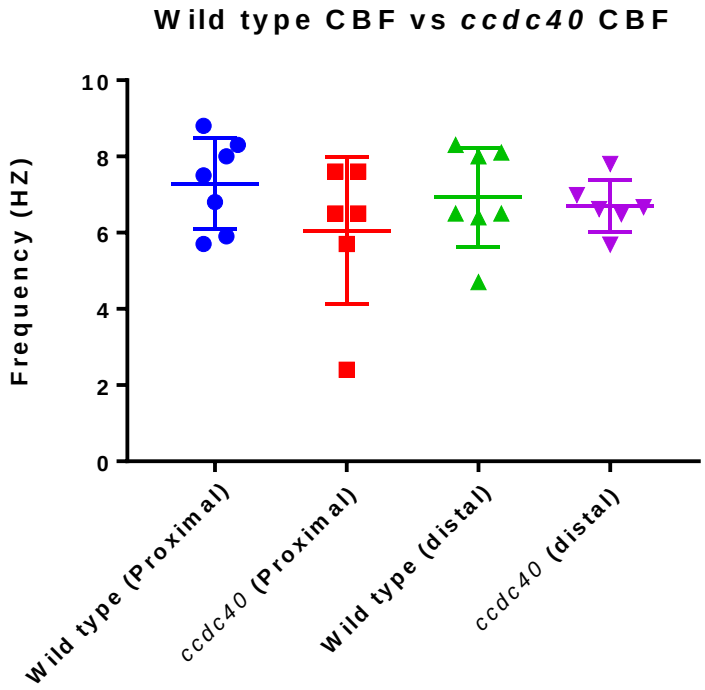

Figure 3.15. Graphical comparison between the proximal and distal zones of wild-type and fish injected with *ccdc40* MO. Scatter plot graphic comparing the proximal zone of wild type fish (n=7) with *ccdc40* injected fish (n=6) measurement of CBF and the distal zone of wild type fish (n=7) with *ccdc40* injected fish (n= 6) measurements of CBF.

The statistical analysis demonstrated that the difference between wild type CBF and *ccdc40* MO injected fish CBF in both proximal and distal regions is not statistically different. Both proximal zone and distal zone, presented *p* values of 0.1855 and 0.7182, respectively. These results were interesting because the injection of the *ccdc40* MO in those fish embryos had caused L-R defects.

4. Discussion

This study started as a follow up of a previous work performed in the lab (Sampaio et al., 2014). Sampaio et al. characterized the importance of flow speed and pattern generated by motile cilia present in Kupffer's vesicle (KV) and its impact in the Left-Right asymmetry establishment. They demonstrated that cilia number and clustering within the KV are crucial for a strong asymmetric flow and establishment of normal *situs*. To achieve these results they had to manipulate cilia motility and generate static cilia. For this purpose they selected to knockdown the *dnah7* gene based on a gene expression study done in the lab (Tavares et al., 2017). Additionally, Zhang et al. (2002) reported that *dnah7* was an important component in the inner dynein arm in human cilia and necessary for motility. With this in mind, *dnah7* MO was successfully used to manipulate cilia motility and its impact was evaluated by measuring the CBF and fluid dynamics in the in KV (Sampaio et al., 2014).

Sampaio et al. demonstrated, through *in situ* hybridization with a *dnah7* RNA probe, that the transcript was present in the KV, in the pronephros and brain ventricles. At 24 hpf other ciliated organs like the posterior tail dorsal region and proximal pronephric tubes also showed *dnah7* expression. Between 24 to 48 hpf *dnah7* appeared in the brain ventricles, otic vesicles and at 48 hpf in the olfactory pits.

The utilization of *dnah7* MO generated several left-right phenotypes. By screening heart and liver orientation in 80 embryos injected with *dnah7* MO, they detected, 44% *situs solidus*, 20% of heterotaxia, 27% *situs inversus* and 9% *situs ambiguous*. The percentage of L-R defects was considerably higher than in the control with 85% of *situs solitus*. Importantly, with immunofluorescence with anti-acetylated alpha tubulin, they validated that the L-R defects were not due to a reduction in the number of cilia or cilia length (Sampaio et al., 2014).

All these results cemented the ground work for my thesis. Although, Sampaio et al. established that the knockdown of *dnah7* could generate totally immotile cilia*,* this work also rouse many questions. The first being, if the phenotypes caused by the *dnah7* MO injections were due to the *dnah7* knockdown or due MO toxicity. Other studies like Schulte-Merker and Stainier (2014) propose alternative methods to test gene function other than MOs, since it is difficult to distinguish between the specific effects of MOs from the non-specific.

The use of CRISPR-Cas9 has been widely spread throughout the scientific community. It became a cheap and versatile tool when compared to other genetic tools available like TALENs or Zinc Finger Nucleases. CRISPR-Cas9 can be implemented in any lab without a big initial investment, and when well established within the laboratory, it can become a very standardized process with a large range of genetic applications. Furthermore, (Hoshijima et al., 2016) among others made compelling arguments for the use of CRISPR for its accessibility and ease of use. With these factors in mind, my goal was to establish a CRISPR-Cas9 protocol for the lab and while doing that validate the phenotype described in (Sampaio et al., 2014). In Summary, it was important to test if the immotile cilia phenotype caused by *dnah7* knockdown was really due to the lack of the *dnah7* protein. For achieving this aim the creation of a *dnah7* mutant line was crucial.

Additionally, so far no patients diagnosed with PCD have been associated with *dnah7* mutations, which made us question what would be the phenotype in humans. Studies from other labs (O'Callaghan et al., 2011),(Li et al., 2016) and (Ben Khelifa et al., 2014) demonstrated that inner dynein arms are necessary for cilia motility and their absence can lead to PCD and infertility in men. Moreover, (O'Callaghan et al., 2011) diagnosed 15 PCD patients that had exclusively inner dynein problems. However, in these patients their cilia were not static. Instead, they were reported to be beating with a stiff beat pattern. It was therefore interesting and important if we could understand if the lack of *dnah7* specifically blocks motility. Hopefully, it will be a matter of time before someone is diagnosed with a mutation in *dnah7*. Meanwhile, we will have the zebrafish mutant line ready to explore and study which might indicate how *dnah7* regulates ciliary motility.

In the present study, screening the SgRNA1 injected embryos for heteroduplexes, indicative of the mutations, yielded a very poor induction rate. Out of the ten pools of eight embryos each, only one pool (batch 1.1) demonstrated heteroduplexes in a PAGE gel. Making the induction rate of SgRNA 1 around 10%. However, this induction rate is probably lower, since it would be highly improbable that all 8 embryos would present heteroduplexes. This can be reinforced by the fact that the heteroduplexes that appeared presented very faint bands meaning that, most likely only one or two embryos from that batch had the mutated DNA, lowering induction rate to 2.5%. The results of SgRNA1 could not be replicated again. As for SgRNA2 injected embryos, the induction rate of mutation was 0%, no heteroduplexes were found in the 8 pools screened. The most likely cause for these poor result is the selection of the SgRNAs used. To try to compensate this lack of results, a third SgRNA was selected, but this SgRNA did not pass from the colony PCR stage, since no positive colonies were detected.

The screening for the progeny of the injected embryos so far did not yield any positive results. Although, the screening was only made to the progeny of 11 embryos, 6 males and 5 females, there are still more 65 fish to be screened in the fish facility. Hopefully, a mutation might be found within these 65 fish. The reasoning behind this low percentage of fish screened was due a combination of events described below.

During the summer of 2016, the fish facility suffered from severe high temperatures, due to bad planning of the air-conditioned unit capacity to cool the fish facility. This resulted in a rise of temperature within the fish facility, meaning that the temperature of the water in the aquariums could not be regulated appropriately. This problem resulted in a severe lowering in the number of postures, and could only be solved after 2 generations of outcrossing our fish lines, that lasted until early 2017, delaying the first step of injecting the SgRNAs.

For this thesis was crucial to start injecting as early and often as possible, since there would be inevitably, a period reserved for the sexual maturation of the crispants (F0) and then of the potential mutants (F1). To worsen this situation, the maturation process also took longer than expected. Pushing the second phase of screen even closer to the deadline. Then, by the time that the crispants started to lay eggs, another unforeseen problem arose, all the reagents necessary for PCR and PAGE had run out and the lab could not place any orders. This occurred due to a change of status of the NOVA University. NOVA Medical School (NMS) had to change into a Foundation and all the ordering platforms changed within our Institute. This lead to a complete block in the NMS financial system and resulted in a total inability

to orders products in all the laboratories from the CEDOC. As a consequence, my work flow was severely impaired.

Nevertheless, if a mutation is still found within the progeny of the fish being raised in the fish facility it would be expectable that these fish would have similar phenotypes to the *dnah7* morphants. Being that *dnah7* encodes for a heavy chain dynein, forming the inner dynein arm. It would be interesting to know if, when *dnah7* is absent, the mutants present immotile cilia or stiff beating cilia.

Studies from (Lindemann and Lesich, 2010) and (Yang, 2006) confirm that both the heavy chain dyneins from the IDAS and the radial spokes are arranged in repeats throughout the axoneme's microtubules, precisely 96 nm spaced apart. Furthermore, (Castleman et al., 2008) says that radial spoke (RS) form a "signal-transduction" between the central pair (CP) and the dynein arms which can regulate dynein induce movement and govern cilia waveform. The link between the radial spoke and inner dyneins arms influences the velocity which the microtubules slide along each other. While the link between the central pair and radial spoke regulates the waveform of the cilia. This regulation of RS and CP form the dynein regulation complex (DRC). DRC is responsible for coordinating the sliding movement between microtubules, but may also coordinate inner arms by ATP inhibition by activating inner arms in a coordinated faction (Porter and Sale, 2000), hence the association between the IDAs and efficient waveform formation. Aside from DRC regulating IDA, (Oda et al., 2013) established that ODA-DRC activity regulates flagellar beating by managing the activity in both ODA and IDAs.

So, there is scope for more regulatory roles of IDAs and it seems that IDAs are an important component in regulatory processes within the cilia. I hypothesize that an absence of *dnah7*, could mean that the link between the radial spokes and inner dyneins arms could disappear resulting in the inability to regulate the IDAs and therefore resulting in phenotype of uncoordinated ciliary beating, reduce mobility and even loss of mobility (as observed by Sampaio et al., 2014).

On the other hand, mutations in radial spoke genes like *rsph4a*, *rsph9* and *rsph1* have been detected in PCD patients (Castleman et al., 2008; Horani and Ferkol, 2016). With this in mind a collaboration between Cilia regulation and disease lab and an Italian group from Pisa led by Mauro Pistello began. In this partnership, the goal was to disrupt *rsph4a* using CRISPR-Cas9. A PhD student initiated the project by selecting three *rsph4a* SgRNAs. To honor the partnership between labs, I continued the project. So far, the only thing left to do before starting injecting, is to linearize the plasmid where the SgRNA was inserted and transcribe the DNA to RNA. If in the future, a mutant line is generated from these SgRNAs, it would be expectable to cause cilia motility defects as has been reported in various studies. The lack of radial spoke would mean that, nothing would be regulating the IDAs and ODAs, since radial spokes are necessary for microtubule sliding regulation in IDAs and are an important component in the DRC that controls overall dynein activity.

Since the study from Sampaio et al. 2014 measured the CBF of *dnah7* morphants it was important to learn how to measure CBF to then compare the CBF from *dnah7* MO injected fish and *dnah7* mutants. Although this was the original plan, it seems that, since last used, the *dnah7* MO became too concentrated and too toxic. When using the same concentration of the MO that Pedro Sampaio used, I

had mortality rates between 50 to 80%. The surviving embryos had severe malformations and none of them seem to be linked to L-R asymmetry defects. It was confirmed that the MO liquid phase evaporated, concentrating the MO and precipitating to non soluble forms. Even injecting a fourth of the original concentration, the mortality rates were extremely high. The idea of using *dnah7* MO was canceled and this MO was replaced by another one this time for the gene *ccdc40* MO.

Mutations in *ccdc40* and *ccdc39* have been found to be a major cause of axonemal disorganization and absent IDAs in PCD patients (Blanchon et al., 2012). It has been proposed that these genes interact with DRC components and are involved in some way in IDAs attachment to the axoneme (Antony et al., 2013). So, because I was interested in the DRC and specifically in inner dynein arm regulation, the use of this morpholino was not out of my main focus.

Gene expression of *dnah7* conducted by Pedro Sampaio during his Master Thesis showed that *dnah7* transcripts were present at the very end of the tail of zebrafish larva with 48 hpf. Since, this same area has many motile cilia in the spinal canal it was interesting to question what would happen to the CBF when comparing controls to *dnah7* MO. Since, *dnah7* MO was toxic it was decided that the CBF analyses would take place in that same region using *ccdc40* MO. Unfortunately, the data obtained would not be as useful, since I detected no differences in the CBF between wild types fish and injected fish with *ccdc40* MO.

Ccd40c has been associated with immotile cilia and even demonstrated L-R defects in the injected embryos. The fact that my results showed that there is no statistical difference between wild type CBF and *ccdc40* CBF makes us question if these particular tail cells express *ccdc40*. All embryos analyzed were screened beforehand for L-R defects and other anomalies, such heart edemas. Since, they all presented defects it would be expected that overall cilia motility would also be impaired, but that was not the case. Some explanations may be hypothesized: 1) since, the CBF analyses were conducted at 48 hpf maybe the MO effect was already gone. However, these effects were still present when cilia in the KV established the L-R asymmetry resulting in L-R defects. 2) Another possible explanation is that those tail cells do not express *ccdc40*. However, there is no literature to back this statement. As future work, an *in situs* hybridization with *ccdc40* could be conducted in that region. If *ccdc40* is not expressed in that region it would be telling us that *ccdc4*0 is not used in all cilia. This would implicate that other factors exist and can replace *ccdc40* in the DRC for the assembly of the radial spokes and IDAs.

As I pioneered the use of CRISPR-Cas9 in the Lab, this Thesis is more technical. However, a lot of ground work was made. At the moment, there is the possibility of having generated a *dnah7* mutant line and the tools are in place for a creation of a *rsph4a* mutant line. In addition, I helped to establish that the software CiliarMove is a valid software also for spinal canal CBF measurements

References

Anderson, R. G. W. The Three-Dimensional Structure of the Basal Body from the Rhesus Monkey Oviduct. *The Journal of Cell Biology* **1972**, *54* (2), 246–265.

Antony, D.; Becker-Heck, A.; Zariwala, M. A.; Schmidts, M.; Onoufriadis, A.; Forouhan, M.; Wilson, R.; Taylor-Cox, T.; Dewar, A.; Jackson, C.; et al. Mutations in CCDC 39 and CCDC 40 Are the Major Cause of Primary Ciliary Dyskinesia with Axonemal Disorganization and Absent Inner Dynein Arms. *Human Mutation* **2013**, *34* (3), 462–472.

Badano, J. L.; Mitsuma, N.; Beales, P. L.; Katsanis, N. The Ciliopathies: An Emerging Class of Human Genetic Disorders. *Annual Review of Genomics and Human Genetics* **2006**, *7* (1), 125–148.

Barbazuk, W. B.; Korf, I.; Kadavi, C.; Heyen, J.; Tate, S.; Wun, E.; Bedell, J. A.; McPherson, J. D.; Johnson, S. L. The Synthenic Relationship of the Zebrafish and Human Genomes. *Genome Research* **2000**, *10*, 1351–1358.

Barrangou, R. CRISPR-Cas Systems and RNA-Guided Interference. *Wiley Interdisciplinary Reviews: RNA* **2013**, *4* (3), 267–278.

Barrangou, R.; Fremaux, C.; Deveau, H.; Richards, M.; Boyaval, P.; Moineau, S.; Romero, D. A.; Horvath, P. CRISPR Provides Acquired Resistance Against Viruses in Prokaryotes. *Science* **2007**, *315* (5819), 1709–1712.

Baxendale, S.; van Eeden, F.; Wilkinson, R. The Power of Zebrafish in Personalised Medicine. In *Advances in Experimental Medicine and Biology*; Advances in Experimental Medicine and Biology; Springer International Publishing: Cham, 2017; Vol. 1007, pp 179–197.

Behan, L.; Galvin, A. D.; Rubbo, B.; Masefield, S.; Copeland, F.; Manion, M.; Rindlisbacher, B.; Redfern, B.; Lucas, J. S. Diagnosing Primary Ciliary Dyskinesia: An International Patient Perspective. *European Respiratory Journal* **2016**, *48* (4), 1096–1107.

Blanchon, S.; Legendre, M.; Copin, B.; Duquesnoy, P.; Montantin, G.; Kott, E.; Dastot, F.; Jeanson, L.; Cachanado, M.; Rousseau, A.; et al. Delineation of CCDC39/CCDC40 Mutation Spectrum and Associated Phenotypes in Primary Ciliary Dyskinesia. *Journal of Medical Genetics* **2012**, *49* (6), 410–416.

Brouns, S. J. J.; Jore, M. M.; Lundgren, M.; Westra, E. R.; Slijkhuis, R. J. H.; Snijders, A. P. L.; Dickman, M. J.; Makarova, K. S.; Koonin, E. V.; van der Oost, J. Small CRISPR RNAs Guide Antiviral Defense in Prokaryotes. *Science* **2008**, *321* (5891), 960–964.

Carte, J.; Wang, R.; Li, H.; Terns, R. M.; Terns, M. P. Cas6 Is an Endoribonuclease That Generates Guide RNAs for Invader Defense in Prokaryotes. *Genes & Development* **2008**, *22* (24), 3489–3496.

Castleman, V. H.; Romio, L.; Chodhari, R.; Hirst, R. A.; de Castro, S. C. P.; Parker, K. A.; Ybot-Gonzalez, P.; Emes, R. D.; Wilson, S. W.; Wallis, C.; et al. Mutations in Radial Spoke Head Protein Genes RSPH9 and RSPH4A Cause Primary Ciliary Dyskinesia with Central-Microtubular-Pair Abnormalities. *American Journal of Human Genetics* **2008**, *84* (2), 197–209.

Chodhari, R.; Mitchison, H. M.; Meeks, M. Cilia, Primary Ciliary Dyskinesia and Molecular Genetics. *Paediatric Respiratory Reviews* **2004**, *5* (1), 69–76.

Deltcheva, E.; Chylinski, K.; Sharma, C. M.; Gonzales, K. CRISPR RNA Maturation by Trans -

Encoded Small RNA and Host Factor RNase III. *Nature* **2011**, *471* (7340), 602–607.
Deveau, H.; Barrangou, R.; Garneau, J. E.; Labonte, J.; Fremaux, C.; Boyaval, P.; Romero, D. A.; Horvath, P.; Moineau, S. Phage Response to CRISPR-Encoded Resistance in Streptococcus Thermophilus. *Journal of Bacteriology* **2008**, *190* (4), 1390–1400.
Doudna, J. A.; Charpentier, E. The New Frontier of Genome Engineering with CRISPR-Cas9. *Science* **2014**, *346* (6213), 1258096–1258096.
Fisch, C.; Dupuis-Williams, P. Ultrastructure of Cilia and Flagella - back to the Future! *Biology of the Cell* **2011**, *103* (6), 249–270.
Fliegauf, M.; Benzing, T.; Omran, H. When Cilia Go Bad: Cilia Defects and Ciliopathies. *Nature Reviews Molecular Cell Biology* **2007**, *8* (11), 880–893.
Goetz, S. C.; Anderson, K. V. The Primary Cilium : A Signalling Centre during Vertebrate Development. *Nature Publishing Group* **2010**, *11* (5), 331–344.
Goldberg, G. W.; Jiang, W.; Bikard, D.; Marraffini, L. A. Conditional Tolerance of Temperate Phages via Transcription-Dependent CRISPR-Cas Targeting. *Nature* **2014**, *514* (7524), 633–637.
Goodenough, U. W. Substructure of Inner Dynein Arms, Radial Spokes, and the Central Pair/projection Complex of Cilia and Flagella. *The Journal of Cell Biology* **1985**, *100* (6), 2008–2018.
Gupta, T.; Mullins, M. C. Dissection of Organs from the Adult Zebrafish. *Journal of Visualized Experiments* **2010**, No. 37, 3–7.
Hatoum-Aslan, A.; Samai, P.; Maniv, I.; Jiang, W.; Marraffini, L. A. A Ruler Protein in a Complex for Antiviral Defense Determines the Length of Small Interfering CRISPR RNAs. *Journal of Biological Chemistry* **2013**, *288* (39), 27888–27897.
Hermans, P. W. M.; Van Soolingen, D.; Bik, E. M.; De Haas, P. E. W.; Dale, J. W.; Van Embden, J. D. A. Insertion Element IS987 from Mycobacterium Bovis BCG Is Located in a Hot-Spot Integration Region for Insertion Elements in Mycobacterium Tuberculosis Complex Strains. *Infection and Immunity* **1991**, *59* (8), 2695–2705.
Hildebrandt, F.; Benzing, T.; Katsanis, N. Ciliopathies. *New England Journal of Medicine* **2011**, *364* (16), 1533–1543.
Hilgendorf, K. I.; Johnson, C. T.; Jackson, P. K. The Primary Cilium as a Cellular Receiver: Organizing Ciliary GPCR Signaling. *Current Opinion in Cell Biology*. 2016, pp 84–92.
Horani, A.; Ferkol, T. W. Primary Ciliary Dyskinesia and Associated Sensory Ciliopathies. *Expert Review of Respiratory Medicine* **2016**, *10* (5), 569–576.
Hoshijima, K.; Jurynec, M. J.; Grunwald, D. J. Precise Editing of the Zebrafish Genome Made Simple and Efficient. *Developmental Cell* **2016**, *36* (6), 654–667.
Ikegami, K.; Setou, M. Unique Post-Translational Modifications in Specialized Microtubule Architecture. *Cell structure and function* **2010**, *35* (1), 15–22.
Ishikawa, H.; Marshall, W. F. Ciliogenesis : Building the Cell ' S Antenna. *Nature Publishing Group* **2011**, *12* (4), 222–234.
Ishikawa, H.; Marshall, W. F. Intraflagellar Transport and Ciliary Dynamics. *Cold Spring Harbor Perspectives in Biology* **2017**, *9* (3), a021998.
Jaffe, K. M.; Thiberge, S. Y.; Bisher, M. E.; Burdine, R. D. Imaging Cilia in Zebrafish. In *Methods in*

Cell Biology; Elsevier Inc., 2010; Vol. 97, pp 415–435.
Jain, R.; Javidan-Nejad, C.; Alexander-Brett, J.; Horani, A.; Cabellon, M. C.; Walter, M. J.; Brody, S. L. Sensory Functions of Motile Cilia and Implication for Bronchiectasis. *Frontiers in bioscience (Scholar edition)* **2012**, *4* (314), 1088–1098.
Jiang, F.; Doudna, J. A. CRISPR–Cas9 Structures and Mechanisms. *Annual Review of Biophysics* **2017**, *46* (1), 505–529.
Jinek, M.; Chylinski, K.; Fonfara, I.; Hauer, M.; Doudna, J. A.; Charpentier, E. A Programmable Dual-RNA-Guided DNA Endonuclease in Adaptive Bacterial Immunity. *Science* **2012**, *337* (6096), 816–821.
Josa, S.; Seruggia, D.; Fernández, A.; Montoliu, L. Concepts and Tools for Gene Editing. *Reproduction, Fertility and Development* **2017**, *29* (1), 1.
Kennedy, M. P.; Omran, H.; Leigh, M. W.; Dell, S.; Morgan, L.; Molina, P. L.; Robinson, B. V.; Minnix, S. L.; Olbrich, H.; Severin, T.; et al. Congenital Heart Disease and Other Heterotaxic Defects in a Large Cohort of Patients With Primary Ciliary Dyskinesia. *Circulation* **2007**, *115* (22), 2814–2821.
Ben Khelifa, M.; Coutton, C.; Zouari, R.; Karaouzène, T.; Rendu, J.; Bidart, M.; Yassine, S.; Pierre, V.; Delaroche, J.; Hennebicq, S.; et al. Mutations in DNAH1, Which Encodes an Inner Arm Heavy Chain Dynein, Lead to Male Infertility from Multiple Morphological Abnormalities of the Sperm Flagella. *American Journal of Human Genetics* **2014**, *94* (1), 95–104.
King, S. M. The Dynein Microtubule Motor. *Biochimica et Biophysica Acta - Molecular Cell Research* **2000**, *1496* (1), 60–75.
King, S. M. Axonemal Dynein Arms. *Cold Spring Harbor Perspectives in Biology* **2016**, *8* (11), 1–12.
Kobayashi, D.; Takeda, H. Ciliary Motility : The Components and Cytoplasmic Preassembly Mechanisms of the Axonemal Dyneins Radial Spokes. *Differentiation* **2012**, *83* (2), S23–S29.
Kuehni, C. E.; Lucas, J. S. Diagnosis of Primary Ciliary Dyskinesia: Summary of the ERS Task Force Report. *Breathe* **2017**, *13* (3), 166–178.
Lai, M.; Pifferi, M.; Bush, A.; Piras, M.; Michelucci, A.; Di Cicco, M.; del Grosso, A.; Quaranta, P.; Cursi, C.; Tantillo, E.; et al. Gene Editing of DNAH11 Restores Normal Cilia Motility in Primary Ciliary Dyskinesia. *Journal of Medical Genetics* **2016**, *53* (4), 242–249.
Li, X.; Heyer, W. D. Homologous Recombination in DNA Repair and DNA Damage Tolerance. *Cell research* **2008**, *18* (1), 99–113.
Li, Y.; Yagi, H.; Onuoha, E. O.; Damerla, R. R.; Francis, R.; Furutani, Y.; Tariq, M.; King, S. M.; Hendricks, G.; Cui, C.; et al. DNAH6 and Its Interactions with PCD Genes in Heterotaxy and Primary Ciliary Dyskinesia. *PLoS Genetics* **2016**, *12* (2), 1–20.
Lieber, M. R. The Mechanism of Human Nonhomologous DNA End Joining. *Journal of Biological Chemistry* **2008**, *283* (1), 1–5.
Lieber, M. R. The Mechanism of Double-Strand DNA Break Repair by the Nonhomologous DNA End-Joining Pathway. *Annual Review of Biochemistry* **2010**, *79* (1), 181–211.
Lindemann, C. B.; Lesich, K. A. Flagellar and Ciliary Beating: The Proven and the Possible. *Journal of Cell Science* **2010**, *123* (4), 519–528.
Lu, Q.; Insinna, C.; Ott, C.; Stauffer, J.; Pintado, P. A.; Rahajeng, J.; Baxa, U.; Walia, V.; Cuenca, A.; Hwang, Y.-S.; et al. Early Steps in Primary Cilium Assembly Require EHD1/EHD3-Dependent Ciliary

Vesicle Formation. *Nature Cell Biology* **2015**, *17* (3), 228–240.
Lucas, J. S.; Barbato, A.; Collins, S. A.; Goutaki, M.; Behan, L.; Caudri, D.; Dell, S.; Eber, E.; Escudier, E.; Hirst, R. A.; et al. European Respiratory Society Guidelines for the Diagnosis of Primary Ciliary Dyskinesia. *European Respiratory Journal*. January 2017, p 1601090.
Makarova, K. S.; Grishin, N. V; Shabalina, S. A.; Wolf, Y. I.; Koonin, E. V. A Putative RNA-Interference-Based Immune System in Prokaryotes: Computational Analysis of the Predicted Enzymatic Machinery, Functional Analogies with Eukaryotic RNAi, and Hypothetical Mechanisms of Action. *Biology direct* **2006**, *1* (1), 7.
Marraffini, L. A. CRISPR-Cas Immunity in Prokaryotes. *Nature* **2015**, *526* (7571), 55–61.
Mojica, F. J. M.; Montoliu, L. On the Origin of CRISPR-Cas Technology: From Prokaryotes to Mammals. *Trends in Microbiology* **2016**, *24* (10), 811–820.
Mojica, F. J. M.; Diez-Villasenor, C.; Soria, E.; Juez, G. Biological Significance of a Family of Regularly Spaced Repeats in the Genomes of Archaea, Bacteria and Mitochondria. *Molecular Microbiology* **2000**, *36* (1), 244–246.
Mojica, F. J. M.; Díez-Villaseñor, C.; García-Martínez, J.; Soria, E. Intervening Sequences of Regularly Spaced Prokaryotic Repeats Derive from Foreign Genetic Elements. *Journal of Molecular Evolution* **2005**, *60* (2), 174–182.
Mushtaq, M. Y.; Verpoorte, R.; Kim, H. K. Zebrafish as a Model for Systems Biology. *Biotechnology and Genetic Engineering Reviews* **2013**, *29* (2), 187–205.
O'Callaghan, C.; Rutman, A.; Williams, G. M.; Hirst, R. A. Inner Dynein Arm Defects Causing Primary Ciliary Dyskinesia: Repeat Testing Required. *European Respiratory Journal* **2011**, *38* (3), 603–607.
Oda, T.; Yagi, T.; Yanagisawa, H.; Kikkawa, M. Identification of the Outer-Inner Dynein Linker as a Hub Controller for Axonemal Dynein Activities. *Current Biology* **2013**, *23* (8), 656–664.
Olivier, K. N.; Sagel, S. D.; Milla, C.; Zariwala, M. A.; Wolf, W. Laterality Defects Other Th an Situs Inversus Totalis in Primary Ciliary Dyskinesia Insights Into Situs Ambiguus and Heterotaxy. *CHEST* **2014**, *146* (5), 1176–1186.
Parng, C.; Seng, W. L.; Semino, C.; McGrath, P. Zebrafish: A Preclinical Model for Drug Screening. *ASSAY and Drug Development Technologies* **2002**, *1* (1), 41–48.
Porter, M. E.; Sale, W. S. The 9 + 2 Axoneme Anchors Multiple Inner Arm Dyneins and a Network of Kinases and Phosphatases That Control Motility. *The Journal of Cell Biology* **2000**, *151* (5), F37–F42.
Prachee Avasthia, W. F. M. Stages of Ciliogenesis and Regulation of Ciliary Length. **2012**, *83* (2), 1–29.
Ran, F. A.; Hsu, P. D.; Wright, J.; Agarwala, V.; Scott, D. A.; Zhang, F. Genome Engineering Using the CRISPR-Cas9 System. *Nat Protoc* **2013**, *8* (11), 2281–2308.
Ritsu Kamiya, Eiji Kurimoto, E. M. Two Types of Chlamydomonas Flagellar Mutants. *Cell* **1991**, *112* (3), 441–447.
Rubbo, B.; Lucas, J. S. Clinical Care for Primary Ciliary Dyskinesia: Current Challenges and Future Directions. *European Respiratory Review* **2017**, *26* (145), 170023.
Samai, P.; Pyenson, N.; Jiang, W.; Goldberg, G. W.; Hatoum-Aslan, A.; Marraffini, L. A. Co-Transcriptional DNA and RNA Cleavage during Type III CRISPR-Cas Immunity. *Cell* **2015**, *161* (5),

1164–1174.
Sampaio, P.; Ferreira, R. R.; Guerrero, A.; Pintado, P.; Tavares, B.; Amaro, J.; Smith, A. A.; Montenegro-Johnson, T.; Smith, D. J.; Lopes, S. S. Left-Right Organizer Flow Dynamics: How Much Cilia Activity Reliably Yields Laterality? *Developmental Cell* **2014**, *29* (6), 716–728.
San Filippo, J.; Sung, P.; Klein, H. Mechanism of Eukaryotic Homologous Recombination. *Annual Review of Biochemistry* **2008**, *77* (1), 229–257.
Sapranauskas, R.; Gasiunas, G.; Fremaux, C.; Barrangou, R.; Horvath, P.; Siksnys, V. The Streptococcus Thermophilus CRISPR/Cas System Provides Immunity in Escherichia Coli. *Nucleic Acids Research* **2011**, *39* (21), 9275–9282.
Sashital, D. G.; Wiedenheft, B.; Doudna, J. A. Mechanism of Foreign DNA Selection in a Bacterial Adaptive Immune System. *Molecular Cell* **2012**, *46* (5), 606–615.
Satir, P.; Christensen, S. T. Overview of Structure and Function of Mammalian Cilia. *Annual Review of Physiology* **2007**, *69* (1), 377–400.
Schulte-Merker, S.; Stainier, D. Y. R. Out with the Old, in with the New: Reassessing Morpholino Knockdowns in Light of Genome Editing Technology. *Development* **2014**, *141* (16), 3103–3104.
Sharples, G. J. The X Philes: Structure-Specific Endonucleases That Resolve Holliday Junctions. *Molecular Microbiology* **2001**, *39* (4), 823–834.
Singla, V. The Primary Cilium as the Cell's Antenna: Signaling at a Sensory Organelle. *Science* **2006**, *313* (5787), 629–633.
Sobkowicz, H. M.; Slapnick, S. M.; August, B. K. The Kinocilium of Auditory Hair Cells and Evidence for Its Morphogenetic Role during the Regeneration of Stereocilia and Cuticular Plates. *Journal of Neurocytology* **1995**, *24* (9), 633–653.
Sorokin, S. Centrioles and the Formation of Rudimentary Cilia by Fibroblasts and Smooth Muscle Cells. *The Journal of Cell Biology* **1962**, *15* (2), 363–377.
Sugrue, K. F.; Zohn, I. E. Mechanism for Generation of Left Isomerism in Ccdc40 Mutant Embryos. *PLoS ONE* **2017**, *12* (2), 1–17.
Sui, W.; Hou, X.; Che, W.; Ou, M.; Sun, G.; Huang, S.; Liu, F.; Chen, P.; Wei, X.; Dai, Y. CCDC40 Mutation as a Cause of Primary Ciliary Dyskinesia: A Case Report and Review of Literature. *The Clinical Respiratory Journal* **2016**, *10* (5), 614–621.
Tavares, B.; Jacinto, R.; Sampaio, P.; Pestana, S.; Pinto, A.; Vaz, A.; Roxo-Rosa, M.; Gardner, R.; Lopes, T.; Schilling, B.; et al. Notch/Her12 Signalling Modulates, Motile/immotile Cilia Ratio Downstream of Foxj1a in Zebrafish Left-Right Organizer. *eLife* **2017**, *6*, e25165.
Verhulst, S. L.; Desager, K.; Van Gaal, L.; De Backer, W. Genotype-Phenotype Correlations in PCD Patients Carrying DNAH5 Mutations. *Journal of Pediatrics*. February 15, 2007, pp 372–373.
Vincensini, L.; Blisnick, T.; Bastin, P. 1001 Model Organisms to Study Cilia and Flagella. *Biology of the Cell* **2011**, *103* (3), 109–130.
Yagi, T.; Minoura, I.; Fujiwara, A.; Saito, R.; Yasunaga, T.; Hirono, M.; Kamiya, R. An Axonemal Dynein Particularly Important for Flagellar Movement at High Viscosity: Implications from a New Chlamydomonas Mutant Deficient in the Dynein Heavy Chain Gene DHC9. *Journal of Biological Chemistry* **2005**, *280* (50), 41412–41420.

Yang, P. Radial Spoke Proteins of Chlamydomonas Flagella. *Journal of Cell Science* **2006**, *119* (6), 1165–1174.

Zariwala, M. A.; Omran, H.; Ferkol, T. W. The Emerging Genetics of Primary Ciliary Dyskinesia. *Proceedings of the American Thoracic Society* **2011**, *8* (5), 430–433.

Zhang, Y. J.; O'Neal, W. K.; Randell, S. H.; Blackburn, K.; Moyer, M. B.; Boucher, R. C.; Ostrowski, L. E. Identification of Dynein Heavy Chain 7 as an Inner Arm Component of Human Cilia That Is Synthesized but Not Assembled in a Case of Primary Ciliary Dyskinesia. *Journal of Biological Chemistry* **2002**, *277* (20), 17906–17915.

Zhu, X.; Liu, Y.; Yang, P. Radial Spokes—A Snapshot of the Motility Regulation, Assembly, and Evolution of Cilia and Flagella. *Cold Spring Harbor Perspectives in Biology* **2017**, *9* (5), a028126.

Annexes

Annex I:

```
Hs      ---------------------------------------TTGCAGGAATTTATAATCAAC    21
Dr      ATTATAAGATGCTTAAGGCCAGACAAGGTTGTTCCAATGGTTCAAGAGTTTGTGTCAGGC    10140
                                              * ** ** *** *      *

Hs      AGATTGGGACGTGCATTCATTGAACCACCCCCCTTTGATTTAGCCAAGGCATTTGGAGAC    81
Dr      AACTTGGGACAGCAGTTTATTGAGGTGCCACCCTTTAATTTGGCCACCGCTTTTGCTGAC    10200
        *  *******     ** *****    ** ****** **** ****  ** ****  ***

Hs      AGTAACTGCTGTGCACCACTGATTTTCGTGCTCTCTCCTGGAGCAGATCCCATGGCTGCC    141
Dr      AGTCACTGCTGCGCTCCGCTCATCTTTATCCTGTCCCCAGGATCAGACCCCATGGCAGCA    10260
        *** ******* ** ** ** ** **  * ** ** ** *** **** ******** **

Hs      CTTCTAAAATTTGCTGATGACCAGGGATATGGGGGATCAAAACTTAGCTCTTTATCTCTT    201
Dr      TTGCTCAAGTTTGGCGAGGAACAGGGCTTCACAGGAAACAGACTGACCTCCCTGTCTCTG    10320
         * ** ** ****  ** ** ***** *     ***   * *** * ***  * *****

Hs      GGTCAAGGCCAAGGGCCCATTGCTATGAAGATGTTAGAAAAAGCTGTCAAGGAAGGAACA    261
Dr      GGACAGGGTCAGGGCCCCATCGCCATGAGCATGATTGAGACTGGTGTGAAGGAAGGAACC    10380
        ** ** ** ** ** ***** ** ****  *** * ** *  * *** ***********

Hs      TGGGTTGTTCTTCAGAATTGTCACCTTGCCACCTCTTGGATGCCAACCCTTGAGAAAGTC    321
Dr      TGGGTAGTTTTACAGAACTGCCACCTGGCCACTTCATGGATGTCCACCCTTGAACGTGTT    10440
        ***** *** * ***** ** ***** ***** ** ****** * ********    **

Hs      TGTGAGGAGTTAAGCCCAGAGTCAACACATCCAGATTTCCGAATGTGGCTAACGAGTTAC    381
Dr      TGTGAGGAGTTGAATGCAGATACCACTCATCCAGACTTCCGCTTGTGGCTGACCAGTTAC    10500
        *********** *   ****  * ** ******** *****  ******* ** ******

Hs      CCATCTCCAAATTTCCCTGTGTCAGTACTGCAGAATGGAGTGAAAATGACCAATGAAGCA    441
Dr      CCGTCTCCCAACTTCCCTGTGGCTGTGCTGCAAAATGGTGTCAAAATGACCAATGAGGCT    10560
        ** ***** ** ********** * ** ***** ***** ** ***************  **

Hs      CCAAAAGGTTTACGGGCTAATATCATTCGATCATACCTCATGGACCCGATCTCTGATCCG    501
Dr      CCCAAGGGGCTGCGCTCCAACATCATCCGTTCTTTCTGCATGGATCCCATATCTGACCCT    10620
        ** ** **  * **  * ** ***** ** ** * *  ****** ** ** ***** **

Hs      GAGTTCTTTGGCAGCTGCAAAAAGCCTGAGGAATTCAAGAAATTGCTTTATGGCCTGTGT    561
Dr      GAGTTTTTTGACAGCAGCTCAAAACCAGCTGTCTTTAAGAAGCTGCTGTTTAGCTTGTGC    10680
        ***** **** **** **  *** ** *  *  ** *****  **** * * ** ****

Hs      TTCTTTCATGCTTTGGTACAAGAAAGACGGAAATTTGGACCCCTAGGGTGGAATATTCCT    621
Dr      TTCTTTCATGCGCTGACGCAAGAGAGAAGGAAATTCGGTCCTCTTGGCTGGAACATTCCC    10740
        ***********  **   ***** *** ******* ** ** ** ** ***** *****

Hs      TATGAGTTCAATGAGACAGATCTGAGAATCAGCGTACAGCAGCTCCACATG---------    672
Dr      TATGAGTTCAACGAGACAGACCTGCGGATCTCTGTCCAGCAGTTACACATGTTCTTGGAC    10800
        *********** ******** *** * ***   ** ****** * ******
```

Figure S1. Alignment of *Homo sapiens dnah7* ATPase region and *danio rerio dnah7* sequences. The sequence comparison was made using Clustal Omega at http://www.ebi.ac.uk/ Tools/msa/clustalo/.

Annex II:

```
Hs      GCAGAAAACGCTCTTCCAAATGTAATGGAGTCAGCTTTTTATTTTGAACAAGCTGGAGTT    60
Dr      GTAGATTCTCCTTTACCCAATGTTGCAGAACTTGCGTTTTTCTTTGAGCAAGCTGGCGTG    60
        * ***     ** * ** *****    **    ** ****  ***** ******** **

Hs      GGTTTGGGCACAGATGAGACATACCGCATATTTCTTGCCCTCAAGCAGCTTACTGATACC    120
Dr      GGTCTGGGGAGAGAGGAGATTCAGAGAATCTTTCTGGCTTTGAAACATCTGGTAGACACA    120
        *** **** * *** ****   *  * ** ***** **  * ** ** **    ** **

Hs      CACCCAATCCAAAGATGCCGCTTCTGGGGAAAGATCTTGGGTCTGGAAATGAATTATATT    180
Dr      CAGCTGCTCTTGCGGTGTCGATTCTGGGGCAAGATCCTTGGGACACAGGGAAACTACCTG    180
        ** *   **    * ** ** ******** ****** * **     *    ** **  *

Hs      GTAGCTGAAGTGGAATTTCGTGAGGGGGAAGATGAAGAGGAAGTGGAAGAGGAAGATGTA    240
Dr      GTGGCGGAAGGGGAATTCAGAGAAGGGGAAGGAGAGGAAGACGAGGGGACAGAACAAA--    238
        ** ** **** ******  * ** *******  ** ** ** * **     *** *

Hs      GCTGAAGAGAGGGACAATGGAGAAAGTGAAGCTCATGAAGATGAGGAAGATGAATTACCA    300
Dr      -CTCCAGAGGAGGACGAGAGAGAGGAAGAGCTGCAGGAGGGCAAGGATGAAGCAGAG---    294
         **  ****  **** *  ****    **    ** ** *   **** ** * *

Hs      AAGTCCTTTTACAAGGCCCCACAGGCTATACCAAAAGAAGAAAGTAGAACAGGTGCCAAC    360
Dr      -----CTTGTGGAGGCT----------------------------------------------    306
             *** *  * *
```

Figure S2. Alignment of *Homo sapiens rsph4a* and *Danio rerio rsph4a* sequences. The sequence comparison was made using Clustal Omega at http://www.ebi.ac.uk/ Tools/msa/clustalo/.

Annex III:

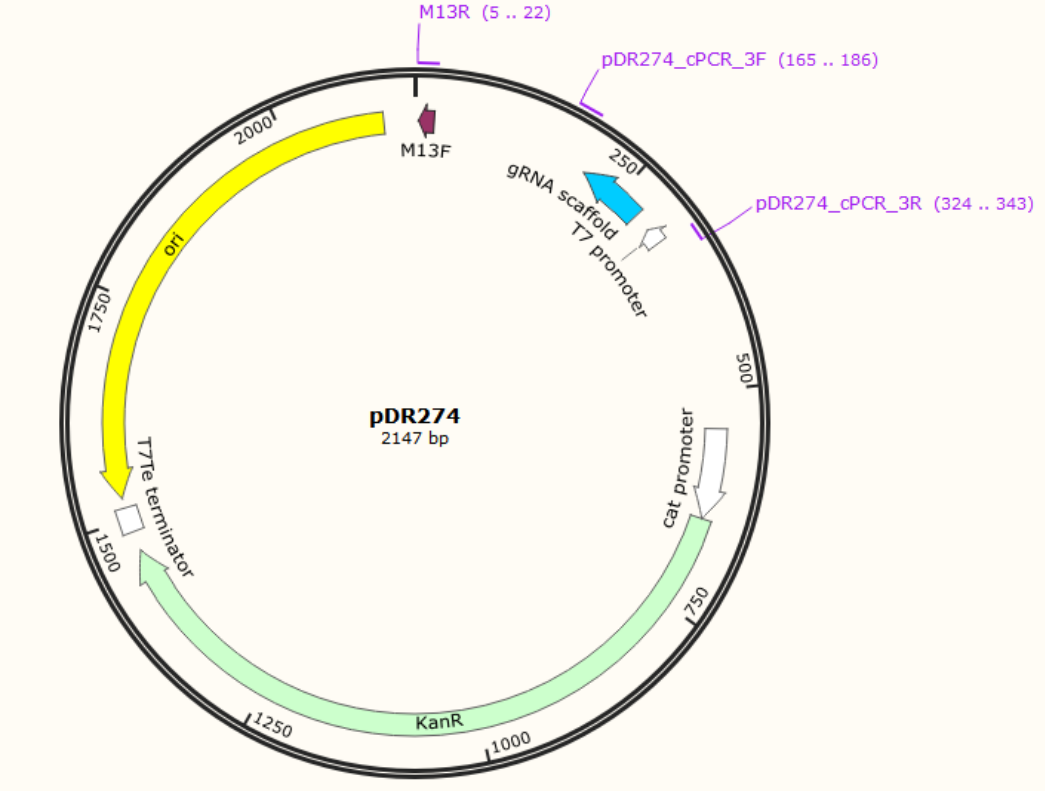

Figure S2. pDR274 plasmid. Pdr274 is a 2174 pb plasmid with an origin of replication (ori), a T7 terminator, a kanamycin resistance with a cat promoter. The plasmid also as an insertion zone, gRNA scaffold accessible with bsaI restriction enzyme. The location of M13F (which is used as a reverse primer), pDR274_Cpcr_3F and pDR274_Cpcr_3R primers. All plasmid modifications were made SnapGene® Viewer 2.8.2. Software (GSL Biotech LLC, Chicago)